PCCP

Accepted Manuscript

This is an *Accepted Manuscript*, which has been through the Royal Society of Chemistry peer review process and has been accepted for publication.

Accepted Manuscripts are published online shortly after acceptance, before technical editing, formatting and proof reading. Using this free service, authors can make their results available to the community, in citable form, before we publish the edited article. We will replace this *Accepted Manuscript* with the edited and formatted *Advance Article* as soon as it is available.

You can find more information about *Accepted Manuscripts* in the Information for Authors.

Please note that technical editing may introduce minor changes to the text and/or graphics, which may alter content. The journal's standard Terms & Conditions and the Ethical guidelines still apply. In no event shall the Royal Society of Chemistry be held responsible for any errors or omissions in this *Accepted Manuscript* or any consequences arising from the use of any information it contains.

ROYAL SOCIETY OF CHEMISTRY

www.rsc.org/pccp

Classification of the mechanisms of photoinduced electron transfer from aromatic amino acids to the excited flavins in flavoproteins

Fumio Tanaka[1,3*], Kiattisak Lugsanangarm[1], Nadtanet Nunthaboot[2], Arthit Nueangaudom[1], Somsak Pianwanit[1], Sirirat Kokpol[1*], Seiji Taniguchi[3], Haik Chosrowjan[3]

[1]Department of Chemistry, Faculty of Science, Chulalongkorn University, Bangkok 10330, Thailand

[2] Department of Chemistry, Faculty of Science, Mahasarakham University, Mahasarakham 44150, Thailand

[3] Division of Laser Biochemistry, Institute for Laser Technology, Utsubo-Honmachi, 1-8-4, Nishiku, Osaka 550-0004, Japan

Abstract

In many flavoproteins a photoinduced electron transfer (ET) efficiently takes place from aromatic amino acids as tryptophan or tyrosine to the excited isoalloxazine, so that the fluorescence lifetimes of isoalloxazine in some flavoproteins become ultrashort. The mechanism of ET in the flavoproteins were classified into four classes from the relationship between logarithmic ET rates (ln Rate) and the donor-acceptor distances (*Rc*), using reported data. A physical quantity, *GT*, was defined as a sum of solvent reorganization energy, electrostatic energy between a donor cation and Iso anion, standard free energy gap between the photoproducts and reactants, and net electrostatic energy between the photoproducts and other ionic groups in the flavoproteins (*NetES*). When *GT* fluctuates around zero with *Rc*, ET rate becomes fastest (faster than 1 ps^{-1}) in Kakitani and Mataga rate. In the ultrafast ET processes the ln Rate becomes parabolic function (Category 1) of *Rc* as in FMN binding proteins and pyranose 2-oxidase at the shorter emission wavelengths, when *NetES* is negligible compared to the other quantities in *GT* function. In the ultrafast ET processes the ln Rate does not display any clear function of *Rc* (Category 2) when *NetES* is dominant in *GT* function, because of no direct relation between *NetES* and *Rc*. ET in flavodoxin from *Helocobacor pylori* may be classified into Category 2. When *GT* linearly varies with *Rc* around a certain positive value, the ET rates become much slower (< 1 ps^{-1}). In this case the ln Rate linearly decreases with *Rc* (Category 3), as Tyr224 in D-amino acid oxidase dimer. It is also conceivable that the ln Rate decreases with much scattered function of *Rc* (Category 4), when *NetES* is dominant in *GT* function, as in Tyr314 in D-amino acid oxidase dimer. In ET processes of Category 1, ET rates decrease as *Rc* becomes shorter than the distance at the maximum values of ln Rate, where *GT* displays negative. Condition and physical meaning were discussed for the *GT*-negative region.

I. Introduction

Flavoproteins play an important role for electron transport, oxidation-reduction reactions in oxidases, oxygenases, dehydrogenases, etc.[1] Photochemistry and photobiology of flavins and flavoproteins are also important fields in science,[2] since a number of new flavin photoreceptors have been found in the last decad.[3] It is considered that initial steps of photo-regulation functions by AppA in photosynthetic systems[4, 5] and TePixD in pili-dependent cell motility[6] are photoinduced electron transfer (ET) from tyrosine (Tyr) to the excited isoalloxazine (Iso*) through hydrogen bonding chain by glutamine. ET phenomena have been central field in photochemistry and photobiology.[7, 8]

Fluorescence of flavins was first observed by Weber.[9] Fluorescence quenching of flavin fluorescence by indole ring was reported with isoalloxazine (Iso) -$(CH_2)_n$-indole compounds by McCormick.[10] Time-resolved fluorescence spectroscopy of flavins and flavoproteins has been reviewed by Berg and Visser.[11] A number of flavoproteins displays practically no fluorescence. However, they emit with very short lifetimes (sub-picoseconds) upon the excitation with an ultra-short pulse laser.[12–16] In these flavoproteins, tryptophan (Trp) and/or Tyr always exist near isoalloxazine ring. The remarkable fluorescence quenching in these flavoproteins was demonstrated to be due to ET from Trp and/or Tyr to the excited Iso (Iso*), by means of picosecond[17, 18] and femtosecond[19] transient absorption spectroscopy.

ET phenomena including dark electron transfer in proteins have been amply reported by many workers during years 1970-2000.[20-29] Moser et al.[25] have experimentally demonstrated linear relationship of the logarithmic ET rates (ln Rate) with the donor-acceptor distances in photosynthetic proteins, which is called the Dutton rule. We have been working on the ET mechanisms in flavoproteins from the aromatic amino acids to Iso* with atomic coordinates

of the proteins determined by molecular dynamics simulation (MDS) and ultrafast fluorescence decays or lifetimes as experimental data.[30-38]

The protein systems dealt in the present work are pyranose 2-oxidase from *Tetrametes multicolor* (P2O), flavodoxin from *Helocobactor pylori* (HPFD), flavin mononucleotide (FMN) binding proteins from *Desulfovibrio vulgaris*, Miyazaki F (FBP), and D-amino acid oxidase from porcine kidney (DAAO). The P2O is a homotetramer (Mw; 67 kDa per subunit), covalently bound flavin adenine dinucleotide (FAD) as a cofactor. It catalyses oxidative degradation of lignin to produce hydrogen peroxide.[39] Crystal structure of wild type P2O has been determined by Kujawa et al.[40] HPFD is a small flavoproteins (Mw; 18 kDa) which contains flavin mononucleotide (FMN) as cofactor, and functions as electron transport among proteins.[41] HPFD is a pathogen for type-B gastritis and peptic-ulcer diseases,[41] and gastric carcinoma.[42] FBP (Mw; 18 kDa) also binds FMN and functions as electron transport like flavodoxins.[43] DAAO (Mw; 39 kDa per monomer) is in an equilibrium state between monomer and dimer at relatively low concentrations,[44] and binds one mole of FAD per monomer. DAAO catalyses oxidative degradation of D-amino acids into corresponding imino compounds, ammonium and hydrogen peroxides. Mammalian DAAO associates with the brain D-serine metabolism and with the regulation of the glutamatergic neurotransmission.[45, 46]

In the present work we have described on a classification of the ET mechanisms from the aromatic amino acids to Iso* in P2O, HPFD, FBPs and DAAO dimer based upon the relationship between the ln Rate and *Rc*, using reported ET rates and related physical quantities.

METHODS OF ANALYSES

Procedure for determination of the ET rate from fluorescence decay of a flavoprotein. Principle of the method to determine ET rates from aromatic amino acids to Iso* in flavoproteins are described in a review article.[47] The procedure is illustrated as a Diagram in Supporting Information. Here the method is outlined below.

1) Time-dependent atomic coordinates are determined by MDS method.
2) ET rates are calculated with appropriate initial values of ET parameters contained in an ET theory. Sometimes the initial ET parameters are taken from the reported works.
3) Fluorescence decays and lifetimes of Iso* in flavoproteins are calculated with the ET rates.
4) Value of chi-square (χ^2) is obtained between the observed and calculated decays or lifetimes.
5) New set of ET parameters are evaluated to get smaller values of the chi-square by the non-linear least square method according to Marquardt algorithm.
6) ET rates are calculated with the new set of ET parameters.
7) The procedures 2) to 6) are repeated to obtain the minimum value of the chi-square.
8) Convergence criteria is that the chi-square does not appreciably decrease from one iteration to the next. Numerically the criteria is determined by an equation, $\left\{\chi^2(k)-\chi^2(k+1)\right\}/\chi^2(k)<\varepsilon$, where $\chi^2(k)$ and $\chi^2(k+1)$ are chi-square at *k-th* and *(k+1)-th* iterations. Normally ε is taken to be 10^{-6}.
9) When the criteria is satisfied, ET rates and related physical quantities are calculated with the best-fit ET parameters.

ET rates from Trp168 to Iso* in P2O.

Method of MDS for P2O is described in the previous work.[38] Original Marcus theory[49-51] has been modified in various ways for ET processes.[52-57] In the present analysis, KM model[55-57]

was used, because it is applicable both for adiabatic and non-adiabatic ET processes, and has been found to satisfactorily reproduce experimental fluorescence decays [30-38] and lifetimes of flavoproteins.[58-63] In P2O the observed fluorescence decays were non-exponential, and expressed with two-exponential decay functions[62,63] (see Table S2 in Supporting Information). The lifetimes of fast component in the wild type P2O is emission-wavelength (λ) dependent, while that of the slow component is emission-wavelength independent, 358 ps. The mean lifetime of the fast component is 88 fs over all emission wavelengths. The method of ET analysis for P2O are described in the previous work (see Supporting Information).[38]

Decomposition of logarithmic ET rate into three terms.

The ln Rate may be decomposed as eq. 1.

$$\ln k_{ET} = \ln EC + \ln SQRT + GTLAM \tag{1}$$

Here

$$\ln EC = \ln \frac{\nu_0}{1+\exp\left\{\beta\ (R_i - R_0)\right\}} \tag{2}$$

$$\ln SQRT = \ln \sqrt{\frac{k_B T}{4\pi\lambda_S}} \tag{3}$$

$$GT = \Delta G^0 - e^2 / \varepsilon_{DA} R\ + \lambda_S + E_{Net} \tag{4}$$

$$GTLAM = -\frac{\left\{GT\right\}^2}{4\lambda_S k_B T} \tag{5}$$

The k_{ET} is ET rate expressed with KM model. The ET rates for P2O are given by eq. S1 for fast component and eq S4 for the slow component (Supporting Information). *EC* is an electronic coupling term. *SQRT* denotes a square root term. *GT* is total free energy gap, and *GTLAM* exponential term, and are dependent on emission wavelength *j* in P2O in the fast component of P2O. Among these quantities *EC* ($\ln EC$) and *SQRT* ($\ln SQRT$) are

emission-wavelength independent even in P2O. In eq 4 the following abbreviations are used; *SFEG* for ΔG^0, *ESDA* for $-e^2/\varepsilon_{DA}R$, *SROE* for λ_S, and *NetES* for E_{Net}.

RESULTS

Protein structure of P2O.

The quaternary structure (tetramer) and local structure near FAD are shown in Fig. S1 (Supporting Information).[48] The Trp168 locates near Iso, and closest to Iso among aromatic amino acids. Ionic amino acids, Glu358, Asp452, Lys91 and Arg472, are located near Iso within 1 nm.[48] Mean *Rc* values between Trp168 and Iso are listed in Table S1 (Supporting Information), which are 0.75 nm in subunit A (Sub A), 0.73 nm in Sub B, 0.76 nm in Sub C and 0.75 nm in Sub D. The distances in aqueous solution obtained by MDS are longer by 0.12 – 0.15 nm than those in crystal structure.

ET rates in P2O.

It was identified that the slow fluorescent component is from Sub A and the fast component with the emission-wavelength dependent lifetimes are from Sub B, Sub C and Sub D[38] (see Table S3 in Supprting Infromation). Free energies related to electron affinity of Iso* determined in the previous work[38] are listed in Table S4 (Supporting Information), ET parameters in Table S5. Mean ET rates from Trp168 to Iso* in Sub A, Sub B, Sub C and Sub D obtained in the previous work are also listed in Table S6. The ET rates of the fast component were 10 - 12 ps^{-1} at 580 nm, 8 - 10 ps^{-1} at 555 nm and 530 nm, 14 – 15 ps^{-1} at 500 nm, and 17.5 ps^{-1} at 480 nm. In the slow component of Sub A, it was 0.003 ps^{-1}.

Relationship between ln Rate and *Rc* in P2O.

Fig. 1 shows the ln Rate vs *Rc* relations in Sub B and Sub D of P2O. The relationships for Sub A and Sub C obtained in the previous work[38] are illustrated in Fig. S2 (Supporting Information). At 530 nm of the emission wavelength the ln Rate linearly decreased with *Rc*

both in Sub B and Sub D. The slope was -5.4 in Sub B and -5.3 in Sub D. At 480 nm the ln Rate vs *Rc* function was parabolic, not linear. Approximate function was Y = -12.98 X^2 + 12.21 X – 4.24, where Y is ln Rate ($\ln k_{ij}^{f}$) and X *Rc*. The ln Rate vs *Rc* relation for Sub A and Sub C are reported in the previous work.[38] In Sub A the values of ln Rate are expressed with a linear function. In Sub C the values of ln Rate are also approximated with linear functions at 580, 555 and 530 nm. However, they were parabolic at 500 and 480 nm. The coefficients of these approximated functions obtained in the previous work[38] are listed in Table S7 (Supporting Information).

Relationship between *GT* and *Rc* in P2O.

Fig. 2 shows dependence of GT on *Rc* in Sub A (emission-wavelength independent), Sub B and Sub D at 530 nm and 480 nm (the fast components). In all systems GT approximately linearly increased with *Rc*. Table 1 lists the slopes of the approximated linear functions and the range of GT. The slopes were 1.52 in Sub A, 1.59 in Sub B, 1.53 in Sub C and 1.39 in Sub D. The slopes did not vary appreciably with the emission wavelength. The GT varied in the ranges of 1.14 – 1.34 in Sub A. In Sub B the variation ranges in GT were 0.15 - 0.37 at 580 nm, 0.20 – 0.43 at 555 and 530 nm, 0.04 – 0.27 at 500 nm, and -0.15 – 0.08 at 480 nm. In Sub C the variation ranges were 0.23 – 0.43 at 580 nm, 0.20 – 0.29 at 555 nm, 0.28 – 0.48 at 530 nm, 0.12 – 0.32 at 500 nm, and -0.07 – 0.13 at 480 nm. In Sub D the ranges were 0.21 – 0.43 at 580 nm, 0.27 – 0.48 at 555 nm, 0.26 – 0.47 at 530 nm, 0.11 – 0.32 at 500 nm and -0.08 – 0.12 at 480 nm. Mean values of *GT* over 25000 snapshots are listed in Table S6 (Supporting Information). In the fast component the range of GT (Table 1) and the mean value of *GT* shifted toward lower values at 500 nm and 480 nm, compared to those at other emission wavelengths (Table S6; Supporting Information). At 480 nm the ranges extended from negative to positive values in all fast subunits, which implies that *GT* values fluctuate around zero.

ET processes in any subunits in P2O are adiabatic, because the values of R_0^f and R_0^s are 1.30 and 1.21 nm (see Table S5, Supporting Information). Accordingly, the values of $\ln EC$ given by eq. 2 are almost constants (see Fig. S5, Supporting Information). Variations of ln *SQRT* given by eq. 3 are shown in Fig. S3 (Supporting Information). Amplitudes of the variation are little and almost constant with time.

Fig. 3 shows relationships between *GTLAM* and *Rc* in Sub B and Sub D of P2O. At 530 nm the *GTLAMs* can be expressed by linear functions of *Rc* both in Sub B and Sub D, while at 480 nm they were approximated with parabolic functions. Behaviour of *Rc*-dependent *GTLAM* in Sub B and Sub D was similar with Sub C (see Fig. S4 in Supporting Information). Coefficients of the approximate functions of *GTLAM* against *Rc* in P2O are given in Table S7. In P2O ET processes are all adiabatic, so that $\ln EC$ terms did not change appreciably with *Rc* (see Fig. S5 in Supporting Information). The slopes of ln Rate vs *Rc* and *GTLAM* vs *Rc* functions are similar. In another word behaviour of ln Rate vs *Rc* relation in P2O are determined by the *GTLAM* vs *Rc* relationships.

Relationships of *GT* and *GTLAM* with *Rc* in HPFD.

Protein structure of HPFD near FMN is shown in Fig. S6 (A) (Supporting Information). ET rates and related physical quantities in HPFD are listed in Table S8 (Supporting Information). In HPFD Tyr91 is fastest ET donor to Iso*among aromatic amino acids.[35] All physical quantities including the ET rate are taken from Ref 35. Fig. 4A shows a relationship of ln *EC* with *Rc* in HPFD. Variation of ln *EC* was little (from 6.365 to 6.395), because ET process of Tyr91 in HPFD is almost adiabatic (R_0 = 1.14 nm, while *Rc* varies from 0.5 to 0.65 nm).[35] Variation of ln *SQRT* was also little with 0.1 width as shown in Fig. 4B. On the other hand the variation of *GT* was quite wide from -0.4 to 0.3 eV as shown in Fig. 4C. Fig. 4D shows dependence of *GTLAM* on *Rc*. The variation range was remarkable from zero to -7. The ln Rate is obtained as a sum of ln *EC*, ln *SQRT*, and *GTLAM* as in eq. 1. The ln Rate vs *Rc*

relationship is shown in Fig. S7 (Supporting Information). Marked fluctuation of *GTLAM* as in Fig. 4D was due to the great variation of *GT* with *Rc* as in Fig. 4C.

Here a quantity, *GP* is defined by eq. 6.

$$GP = SROE + ESDA + SFEG \tag{6}$$

Here $SROE$ is solvent reorganization energy as noted below eq 5 (see also eqs. S2 and S5 for P2O in Supporting Information), $ESDA$, ES energy between Iso anion and donor cation, *SFEG* (eqs. S3 and S6 for P2O in Supporting Information), standard free energy gap.

$SROE + ESDA$ in *GT* or GP varies with *Rc* as eq.7.

$$SROE + ESDA = e^2\left(\frac{1}{2a_{Iso}} + \frac{1}{2a_q}\right)\left(\frac{1}{\varepsilon_\infty} - \frac{1}{\varepsilon_{DA}}\right) - \frac{e^2}{\varepsilon_\infty R_c} \tag{7}$$

Hence *GP* in eq. 6 and *GT* in eq. 4 increases linearly with *Rc* (more exactly, hyperbolic function of *Rc*), because *SFEG* term (eqs. S3 or S6 for P2O in Supporting Information) and *Rc* in eq. S8 for P2O (Supporting Information) are independent of *Rc* in the present model.

Then why *GT* displayed remarkable fluctuation with *Rc* in HPFD? Fig. 5 shows dependence of each component in *GT* on *Rc*. The *SROE* and *ESDA* increased with *Rc* (Figs. 5A and 5B). This is natural because the both terms vary with 1 / *Rc*. In fact *SROE* + *ESDA* increases with *Rc* as eq. 7. The *Rc*-dependence of *GP,* which is a sum of *SROE*, *ESDA* and *SFEG* ($\Delta G^0_{Tyr91} = E^{Tyr}_{IP} - G^0_{Iso} = 0.841$ eV[35]) as in eq. 7, is shown in Fig. 5C. It is noted that the values of *GP* in eq. 6 varies around zero with *Rc*. The *NetES* also vary around zero with *Rc* as in Fig. 5D, but the variation amplitude was much greater than that of *GP*. The *NetES* does not have any explicit relation with *Rc*, so that it markedly fluctuates with *Rc*. This is the reason why the *GT* markedly fluctuates with *Rc*, since sum of *GP* and *NetES* is equal to *GT* (see eq. 4).

Relationship between *GT* and *Rc* in FBPs.

Protein structures of wild type (WT) FBP, E13K (Glu13 is replaced by Lys) FBP, E13R (Glu13 is replaced by Arg) FBP, E13T (Glu13 is replaced by Thr) FBP and E13Q (Glu13 is replaced by Gln) FBP are shown in Fig. S8 (Supporting Information). In FBPs Trp32, Tyr35 and Trp106 are plausible ET donors. *Rc*s to Iso are ca. 0.66 - 0.75 nm in Trp32, 0.85 - 1.0 nm in Tyr35 and 0.91 – 1.05 nm Trp106.[36] Distances between the amino acid residue-13 and Iso were around 1.5 nm, while between the amino acid residue-13 and Trp32, Tyr35 and Trp106 they were around 1.0 nm, 1.2 nm and 1.8 nm, respectively.[36] Best-fit ET parameters are listed in Table S9 (Supporting Information). ET rates calculated from the best-fit ET parameters are listed in Table S10[37] (Supporting Information). The ET rates are fastest from Trp32. The rate from Trp32 were 6.11 in WT, 8.65 in E13K, 8.25 in E13R, 6.70 in E13T and 5.02 ps^{-1} in E13Q. Physical quantities of Trp32 as *NetES* , *SROE*, *ESDA*, and *SFEG* (ΔG^0_{Trp}) are listed in Table S11 (Supporting Information).

Relationship between *GT* and *Rc* are shown in Fig. 6. *GTs* increased with *Rc*, which were approximated with linear functions. The coefficients of the linear functions (Y = A X + B) are listed in Table 2, where Y is *GT* and X is *Rc*. The values of A were 1.49 in WT, 1.96 in E13K, 2.35 in E13R, 1.75 in E13T and 1.56 in E13Q.

Relationships of *GTLAM* with *Rc* and ln Rate with *Rc* in FBPs.

Dependences of *GTLAM* on *Rc* in five FBP isoforms are shown in Fig. 7. In the all isoforms the *GTLAM* could be approximated with parabolic functions, $Y = A X^2 + B X + C$, where Y is *GTLAM* and X is *Rc*. The coefficients, A, B, and C, are listed in Table 2. In Table 2 the coefficients in the parabolic functions of ln Rate with *Rc* are also listed for comparison.[36] The coefficient of A in *GTLAM* vs *Rc* function was considerably larger than that of A in ln Rate vs *Rc* function in the every isoform, whereas the B coefficient in *GTLAM* vs *Rc* function was much smaller than the B coefficient in ln Rate vs *Rc* function. The result reveals that ET mechanisms in the FBP isoforms are quite different from those in the fast component at 500

nm and 480 nm of the emission wavelength in P2O (see Table S7; Supporting Information), where every coefficient in the parabolic function are similar between those in ln Rate vs *Rc* function and *GTLAM* vs *Rc* function. The difference in the ET mechanisms is ascribed to different dependencies of ln *EC* term on *Rc* between FBPs and P2O. Fig. 8 shows relationship between ln *EC* vs *Rc* in five FBPs. In the FBP isoforms ln *EC* term appreciably decreased with *Rc*, whereas in the fast component at 500 and 480 nm in P2O did not depend on *Rc*. If eq. 1 is taken into account, ln *EC* considerably contributes to ln Rate in FBP isoforms.

***Rc*-dependencies of ln Rate, *GTLAM* and *GT* in DAAO dimer.**

Best-fit ET parameters to calculate ET rates are listed in Table S12[60] (Supporting Information). Fastest ET rates in DAAO dimer are Tyr224 at 10 °C in Sub A and at 30 °C in Sub B, and Tyr314 at 10 °C in Sub B and at 30 °C in Sub A.[60] *Rc*-dependencies of ln Rate, *GTLAM* and *GT* were examined for Tyr224 and Tyr314 using the MDS snapshots. Fig. 9A, 9B and 9C show the relationships between ln Rate and *Rc*, between *GTLAM* and *Rc*, and between *GT* and *Rc* in Tyr224 at 10 °C in Sub A. Red lines indicate approximate linear functions, of which are represented as Y = A X + B, and X is *Rc* in nm unit, Y is ln Rate in A, *GTLAM* in B and *GT* in eV unit in C, as shown in the inserts. In the inserts coefficients of determination for the linear functions (R^2) are also indicated. The values of R^2 should be 1 when the data of Y and X are completely linear, and zero when the data show no linear relation at all. In the all relationships the values of R^2 were quite high (> 0.6) in Tyr224, which suggests that the linear functions are good approximations. Similar relations for Tyr314 are shown in Fig. 10A, 10B and 10C. Apparently, the linear relations in Tyr314 are poor for the three quantities, ln Rate, *GTLAM* and *GT*. In fact the values of R^2 were all very small (0.18 in ln Rate, 0.0001 in *GTLAM* and 0.0008 in *GT*), compared to those in Tyr224. In *GTLAM* and *GT* the slopes were almost zero. In the other temperature and subunit the slope

(A value) and the R^2 values are listed in Table 3. The R^2 values of *GTLAM* and *GT* were all little in Tyr314 at 10 °C in Sub B, at 30 °C in Sub A and Sub B, and also in Tyr224 at 30 °C in Sub A. In these cases the slopes of ln Rate vs *Rc* functions were all less than -9, while in the other cases the slopes were greater than -14. Especially the slopes in Tyr314 at 10 °C in Sub A and at 30 °C in Sub A were -6.2 and -6.4, respectively, which were very close to $-\beta^{Tyr}$ [60] (6.25 nm^{-1}). These results suggest that the contribution of *GTLAM* to the ln Rate vs *Rc* relation is negligible when *GT* (and *GTLAM*) do not display any linear relation with *Rc*, so that the slope of the ln Rate vs *Rc* function should be close to $-\beta^{Tyr}$. Then why *GT* does not display any linear relation with *Rc* in some cases? As described at HPFD section (see Fig. 5D), *NetES* does not show any direct relation with *Rc*. Accordingly, *GT* in eq. 4 may not display any linear relation with *Rc*, when 1) *GP* in eq. 6 is close to zero, 2) *NetES* is dominant among four quantities in *GT*, 3) if *NetES* displays slight negative slope with *Rc*, then it may be cancelled with the linear function of *GP* vs *Rc* (it always shows a positive slope). In the case of Tyr314 in Sub A (at both 10 °C and 30 °C), *GT* did not display appreciable *Rc*-dependence due to the reason 3) above, because the slopes of *GP* vs *Rc* functions were 0.56 at 10 °C and 0.60 at 30 °C, while the slopes of *NetES* vs *Rc* plots were -0.51 at 10 °C and -0.53 at 30 °C. Accordingly, the slopes of the both approximate linear functions were cancelled out against *Rc*.

Classification of the mechanism of ET in flavoproteins from the relationship between the ln Rate and *Rc*.

ET mechanism in flavoproteins may be classified from two points of view, A) *GT* function, and B) *NetES*. When *GT* varies with *Rc* around zero and further *NetES* is negligible compared to *GP*, the ln Rate display a parabolic function of *Rc*. If *NetES* is not negligible compared to *GP* and *GT* varies with *Rc* around zero, then the ln Rate do not display linear nor parabolic function of *Rc*, and scattered with *Rc*. When *GT* varies with *Rc* around a positive value, ET

rates becomes much slower than those in the above cases, because *GTLAM* values are always negative (see eqs. 1 and 5). Accordingly, there should be four classes as follows: 1) *GT* (eq. 4) varies around zero, and *NetES* is negligible compared to absolute values of *GP*, 2) *GT* varies around zero, and *NetES* is dominant compared to absolute values of *GP*, 3) *GT* varies around a positive value, and *NetES* is negligible compared to absolute values of *GP*, and 4) *GT* varies around a positive value, and *NetES* is dominant compared to absolute values of *GP*. Table 4 shows criteria of the four categories, and examples in the flavoproteins. In Table 4 adiabatic and non-adiabatic ET processes are separately considered for ln Rate vs *Rc* function, and the slopes are shown when the approximate functions are linear.

DISCUSSION

The donor-acceptor distance has been considered to be most influential parameter upon ET rates.[20-29] In the present work the individual parameter has been determined by means of the non-linear least squares methods, using MDS snapshots and fluorescence decays or fluorescence lifetimes as experimental data. Now it is possible to ponder on the ET mechanisms in flavoproteins from the ET parameters thus obtained. Maximum ET rates are obtained when the exponential term is zero, because this term always reduces the ET rates due to its negative sign (*GTLAM,* see eq. 5). When *GT* varies around zero, *GTLAM* becomes a parabolic function of *Rc* (*GP* » *NetES*) or no relation with *Rc* (*GP* « *NetES*). These conditions correspond to Categories 1) and 2), respectively (see Table 4). ET processes classified as Category 1) are found in ET from Trp168 to Iso* in P2O in adiabatic process, and ET from Trp32 to Iso* in FBP isoforms in non-adiabatic processes. The ET from Tyr91 to Iso* in HPFD may be classified as Category 2), because no clear relation was found between ln Rate and *Rc*. A peak *Rc* may be defined as *Rc* with the peak value of ln Rate. When *GT* varies around a certain positive value, ET rates become much slower than those in

Categories 1) and 2). In P2O ET from Trp168 to Iso* in the slow subunit, and in the fast subunits at 530 nm, 555 nm and 580 nm of the emission wavelength in P2O. Here ET processes are adiabatic and classified as Category 3). ET processes from Tyr35 to Iso* in FBP isoforms were mostly non-adiabatic and also classified as Category 3). ET processes from Tyr224 and Tyr314 to Iso* in DAAO dimer were also non-adiabatic, but the ln Rate vs *Rc* function was much scattered though ln Rate decreased with *Rc*, because the values of *NetES* were not negligible compared to *GP*. ET in this case may be also classified as Category 3), while in ET process from Tyr314 in DAAO dimer the linear relationship between ln Rate and *Rc* were not clear due to dominant *NetES* compared to *GP* which may be classified as Category 4). The slopes of the linear functions in ln Rate vs *Rc* are determined by the slopes ($-S_g$ in Table 4) of *GTLAM* vs *Rc* functions in adiabatic ET processes, while the slopes in ln Rate vs *Rc* functions may be expressed as sums of the slopes in *GTLAM* vs *Rc* function ($-S_g$) plus $-\beta^w$ (w is Trp or Tyr) in *EC* term. The linear relations[25] may hold in Categories 3) and 4) in the present model.

In the previous work[36] it was pointed out that KM rate is not valid anymore in the region of *Rc* where *GT* is negative, because ET rate decreases with decreasing *Rc*, despite that the interaction energy between the donor and acceptor should increase with decreasing *Rc*. It is of interest to discuss more in detail on the negative region of *GT* in Category 1), where the *NetES* is negligible compared to *GP*. Then *GT* is nearly equal to *GP*. The condition for the negative *GT* may be expressed as eq. 8 in KM rate.

$$\frac{e^2}{\varepsilon_\infty R_c} + G^0_{Iso} > e^2\left(\frac{1}{2a_{Iso}} + \frac{1}{2a_q}\right)\left(\frac{1}{\varepsilon_\infty} - \frac{1}{\varepsilon_{DA}}\right) + E^q_{IP} \qquad (8)$$

The negative values of *GT* may be attained when 1) R_c is quite short, 2) G^0_{Iso} (electron affinity of Iso*) is greater than E^q_{IP} (ionization potential of a donor q), 3) ε_{DA} is close to ε_∞.

The charge transfer complexes between Trp32 and Iso* in FBP,[65] and between Trp59 or Tyr97 and Iso*[66] were studied by a semi-empirical molecular orbital method. In these systems the charge transfer interactions are considered to take place in *GT*-negative region. It is also worthy to discuss on a charge transfer complex and ET phenomena between N,N'-dimethylaniline (DMA) and the excited pyrene (Py*) in DMA-$(CH_2)_n$-pyrene diads.[64] The fluorescence from the charge transfer complex between DMA and Py* in the diads was observed only in non-polar solvents, and instead a transient absorption band of pyrene anion in polar solvents was observed as a consequence of ET from DMA to the Py*.[64] In the charge transfer complex, the conditions of 1) and 3) may be fulfilled, and accordingly the interaction between DMA and Py* in the charge transfer complex should be quantum chemically dealt. From a classical view the transferred electron from DMA to Py* could take place recombination to the donor cation from pyrene anion, and from the donor to Py* again, which forms a kind of equilibrium state as the charge transfer complex. As *Rc* increases a potential surface of Iso* could intersect with that of a charge separation state, and so the charge separation could occur at *Rc* longer than the intersection distance.

CONCLUSION

Not only electronic coupling term but also nuclear term play an important role on the ln Rate vs *Rc* relations. The ln Rate vs *Rc* function is linear or parabolic or noisy without any clear relations in ET processes from aromatic amino acids to Iso* in flavoproteins. The behaviour was classified into four Categories with *GP* and *NetES* quantities. When *GT* quantity fluctuates around zero, ET rates are ultrafast (< 1 ps^{-1}). In this case ln Rate vs *Rc* function becomes a parabolic when *GP* > *NetES* (Category 1), no clear function (Category 2) when *GP* < *NetES*. When *GT* fluctuates around a positive values, the ET rate becomes much slower than 1 ps^{-1}. In this case case the ln Rate vs *Rc* function becomes a linear function when *GP* <

NetES (Category 3). It is also no clear function when *GP* < *NetES* (Category 4), even though the ET rate is slow.

Reference

1 *Flavins and Flavoproteins 2008*, ed. by S. Frago, C. Gomez-Moreno, M. Medina, Prensas Universitarias de Zaragoza, 2009.

2 *Flavins: Photochemistry and Photobiology*, ed. by E. Silva, A. M. Edwards, *RC*S Publishing, 2006.

3 Crosson, S., Moffat, K., *Proc. Natl. Acad. Sci. U.S.A.* , 2001, 98, 2995-3000.

4 Masuda, S., Bauer, C. E., *Cell*, 2002, 110, 613-623.

5. M. Gauden, S. Yeremenko, W. Laan, I.H.M. van Stokkun, I.J.A. Ihalainen, R. van Grondelle, K.J. Hellingwerf, J.T.M. Kennis, Biochemistry 2005, 44, 3653–3662.

6. A. Kita, K. Okajima, Y. Morimoto, M. Ikeuchi, K. Miki, J. Mol. Biol. 2005, 349, 1–9.

7 Jortner, J., Bixon, M., eds., *Advances in Chemical Physics*, *Electron Transfer—From Isolated Molecules to Biomolecules*, Wiley-Interscience, New York, 1999.

8 Mataga, N., Chosrowjan, H., Taniguchi, S., *J. Photochem. Photobiol. C* 2005, 6, 37-79.

9 G. Weber, G., *Biochem. J*., 1950, 47, 114-121.

10 McCormick, D. B., *Photochem. Photobiol*., 1977, 26, 169-182.

11 van der Berg, P. A., Visser, A. J. W. G., in *New Trends in Fluorescence Spectroscopy Applications to Chemical and Life Sciences*, Valeur, B., Brochon, J. C., Eds., Springer, Berlin, 2001, pp. 457-485.

12 Mataga, N., Chosrowjan, H., Shibata, Y., Tanaka, F., *J. Phys. Chem. B*, 1998, 102, 7081-7084.

13 Mataga, N., Chosrowjan, H., Shibata, Y., Tanaka, F., Nishina, Y., Shiga, K., *J. Phys. Chem. B*, 2000, 104, 10667-10677.

14 Mataga, N., Chosrowjan, H., Taniguchi, S., Tanaka, F., Kido, N., Kitamura, M., *J. Phys. Chem. B*, 2002, 106, 8917-8920.

15 Chosrowjan, H., Taniguchi, S., Mataga, N., Tanaka, F., Todoroki, D., Kitamura, M., *J. Phys. Chem. B*, 2007, 111, 8695-8697.

16 Chosrowjan, H., Taniguchi, S., Mataga, N., Tanaka, F., Todoroki, D., Kitamura, M., *Chem. Phys. Lett.*, 2008, 462, 121-124.

17 Karen, A., Ikeda, N., Mataga, N., Tanaka, F., *Photochem. Photobiol.,* 1983, 37, 495-302.

18 Karen, A., Sawada, M. T., Tanaka, F., Mataga, N., *Photochem. Photobiol*., 1987, 45, 49-53.

19 Zhong, D. P., Zewail, A. H., *Proc. Natl. Acad. Sci. U. S. A.*, 2001, 98, 11867-11872.

20 Hopfield, J. J., *Proc. Nat. Acad. Sci. USA*, 1974, 71, 3640-3644.

21 Ma*Rc*us, R. A., Sutin, N., *Biochim. Biophys. Acta*, 1985, 811, 265–322.

22 Warshel, A., Chu, Z. T., Parson, W.W., *Science*, 1989, 246, 112-116.

23 Warshel, A., Parson, W.W., *Rev. Phys. Chern*. 1991,42, 279-309.

24 Beratan, D. N., Betts, J. N., Ounchic, J. N., *Science*, 1991, 252, 1285-1288.

25 Moser, C., Keske, J., Warncke, K., Farid, R., Dutton, P. Nature, 1992, 355, 796–802.

26 Bendall, D. S. *Protein Electron Transfer*. BIOS Scientific Publishers Ltd., Oxford, UK, 1996.

27 Gray, H. B., Winkler, J. R., *Annu. Rev. Biochem.*, 1996, 65, 537-561.

28 Warshel, A., Parson, W.W., *Quart. Rev. Biophys*. 2001, 34, 563–679.

29 Biophysics of Electron Transfer and Molecular Bioelectronics (Electronics and Biotechnology Advanced (Elba) Forum Series), Nicolini, C., Editor, Springer, (1999).

30 Nunthaboot, N., Tanaka, F., Kokpol, S., Chosrowjan, H., Taniguchi, S., Mataga, N., *J. Photochem. Photobiol., A*, 2009, 201, 191-196.

31 Nunthaboot, N., Tanaka, F., Kokpol, S., Chosrowjan, H., Taniguchi, S., Mataga, N., *J. Phys. Chem. B*, 2008, 112, 13121-13127.

32 Lugsanangarm, K., Pianwanit , S., Kokpol, S., Tanaka, F., Chosrowjan ,H., Taniguchi, S., Mataga, N., *J. Photochem. Photobiol. A*, 2011, 219, 32-41.

33 Lugsanangarm , K., Pianwanit , S., Kokpol, S., Tanaka, F., Chosrowjan, H., Taniguchi, S., Mataga, N., *J. Photochem. Photobiol. A,* 2011, 219*,* 32–41.

34 Nunthaboot, N., Pianwanit, S., Kokpol, S., Tanaka, F., *Phys. Chem. Chem. Phys*., 2011, 13, 6085-6097.

35 Lugsanangarm, K., Pianwanit, S., Nueangaudom, A., Kokpol, S., Tanaka, F., Nunthaboot, N., Ogino, K., Takagi, R., Nakanishi, T., Kitamura, M., Taniguchi, S., Chosrowjan, H., *J. Photochem. Photobiol. A*, 2013, 268, 58-66.

36 Nunthaboot, N., Lugsanangarm, K., Pianwanit, S., Kokpol, S., Tanaka, F., Taniguchi, S., Chosrowjan, H., Nakanishi, T., Kitamura, M., *Comp. Theor. Chem.* 2014, 1030, 9-16.

37 Nunthaboot, N., Lugsanangarm, K., Nueangaudom, A., Pianwanit, S., Kokpol S., Tanaka, F., Mol. Sim.*,* published on line, DOI: 10.1080/08927022.2014.902534.

38 Lugsanangarm, K., Nueangaudom, A., Kokpol, S., Pianwanit, S., Nunthaboot, N., Tanaka, F., Taniguchi, S., Chosrowjan, H., Submitted.

39 Leitner, C., Volc, J., Haltrich, D., *Appl. Environ. Microbiol.* 2001, 67, 3636 – 3644.

40 Kujawa M., Ebner H., Leitner C., Hallberg B.M., Prongjit M., Sucharitakul J., Ludwig R., Rudsander U., Peterbauer C., Chaiyen P., Haltrich D., Divne C., *J. Biol. Chem.* 2006, 281, 35104-35115.

41 Blaser, M. J., *Gastroenterology* 1992, 102*,* 720–727.

42 Nomura, A., Stemmermann, G. N., Chyou, P. H., Kato, I., Perez-Perez, G. I., Blaser, M. J., Engl. N., *J. Med.* 1991, 325, 1132–1136.

43 Kitamura, M., Kojima, S., Ogasawara, K., Nakaya, T., Sagara, T., Niki, K., Miura, K.,Akutsu H., Kumagai, I., *J. Biol. Chem.*, 1994, 269, 5566-5573.

44 Yagi K & Ohishi N, *J. Biochem. (Tokyo)*, 1972, 71, 993-998.

45 Madeira, C., Freitas, M. E., Vargas-Lopes, C., Wolosker, H., Panizzutti, R., *Schizophr. Res.* 2008, 101, 76-83.

46 Boks, M. P. M., Rietkerk, T., van de Beek, M. H., Sommer, I. E., de Koning, T. J., Kahn, R. S., *Eur. Neuropsychopharmacol*. 2007, *17*, 567-572.

47 Nunthaboot, N., Lugsanangarm, K., Nueangaudom, A., Pianwanit, S., Kokpol, S., Tanaka, F.*, in Fluorescence Spectroscopy and Microscopy, Methods and Protocols,* Engelborghs, Y., Visser, A. J. W. G., Editors, Humana Press (Springer), New York, pp 337-355, 2014.

48 Lugsanangarm, K., Kokpol, S., Nueangaudom, A., Pianwanit, S., Nunthaboot, N., Tanaka, F., *J. Theor. Comp. Chem.* 2014, 13: DOI: 10.1142/S0219633614400100.

49 Ma*Rc*us, R. A., *J. Chem. Phys*., 1956, 24, 966-978.

50 Ma*Rc*us, R. A., *J. Chem. Phys.* 1956, 24, 979-989.

51 Ma*Rc*us, R. A., *Annu. Rev. Phys. Chem*., 1964, 15*,* 155-196.

52 Bixon, M., Jortner, J., *J. Phys. Chem.,* 1991, 95, 1941-1944.

53 Bixon, M., Jortner, J., *J. Phys. Chem*., 1993, 97,13061-13066,.

54 Bixon, M., Jortner, J., J. Cortes, J., Heitele, H., Michel-Beyerle, M. E., *J. Phys. Chem*., 1994, 98, 7289-7299.

55 Kakitani, T., Mataga, N., *J. Phys. Chem.* 1985, *89*, 8-10.

56 Kakitani, T., Yoshimori, A., Mataga, N., *in Advances in Chemistry Series*, Bolton, J. R., Mataga, N., McLendon, G., Eds., American Chemical Society, Washington, DC, 1991, vol. 228, pp. 45-69.

57 Matsuda, N., Kakitani, T., Denda, T., Mataga, N., *Chem. Phys.*, 1995, 190, 83-95.

58 Chosrowjan, H., Taniguchi, S., Mataga, N., Nakanishi, T., Haruyama, Y., Sato, S., Kitamura, M., Tanaka, F., *J. Phys. Chem. B*, 2010, 114, 6175-6182.

59 Taniguchi, S., Chosrowjan, H., Tanaka, F., Nakanishi, T., Sato, S., Haruyama, Y., Kitamura, M., *Bull. Chem. Soc. Japan*. 2013, 86, 339-350.

60 Nueangaudom, A., Lugsanangarm, K., Pianwanit, S., Kokpol, S., Nunthaboot N., Tanaka, F., *Phys. Chem. Chem. Phys.*, 2014, 16, 1930-1944.

61 Nueangaudom, A., Lugsanangarm, K., Pianwanit, S., Kokpol, S., Nunthaboot, N., Tanaka, F., *Phys. Chem. Chem. Phys.*, 2012, 14, 2567-2578.

62 Chosrowjan, H., Taniguchi, S., Wongnate, T., Sucharitakul, J., Chaiyen, P., Tanaka, F., *J. Photochem. Photobiol. A*, 2012, 234, 44–48.

63 Taniguchi, S., Chosrowjan, H., Wongnate, T., Sucharitakul , J., Chaiyen, P., Tanaka, F., *J. Photochem. Photobiol. A*, 2012, 245, 33– 42.

64 Okada, T., Migita, M., Mataga, N., Sakata, Y., Misumi, S., *J. Am. Chem. Soc.,* 1981, 103, 4715-4720.

65. N. Nunthaboot, F. Tanaka, S. Kokpol, H. Chosrowjan, S. Taniguchi, N. Mataga, *J. Phys. Chem. B*, 2008, 112, 15837–15843.

66. K. Lugsanangarma, S, Pianwanita, S. Kokpol, F. Tanaka, H. Chosrowjan, S. Taniguchi, N. Mataga, *J. Photochem. Photobiol. A*, 2011, 217, 333–340.

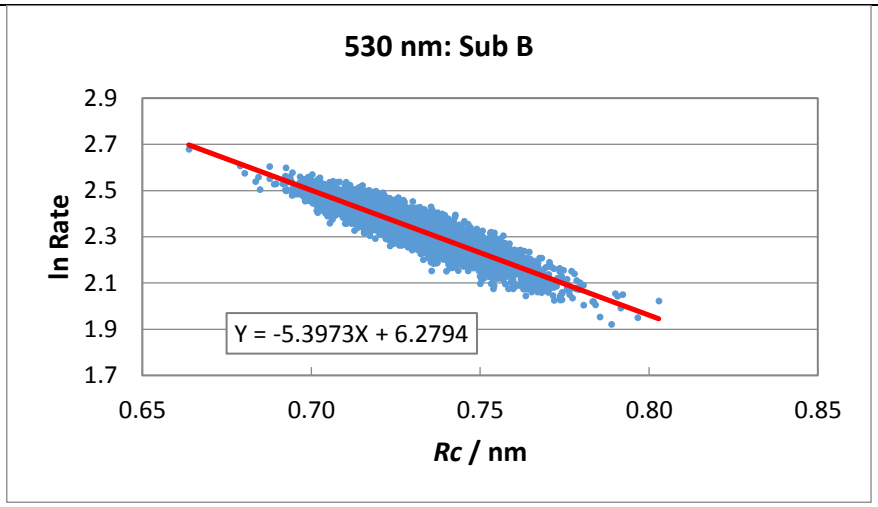

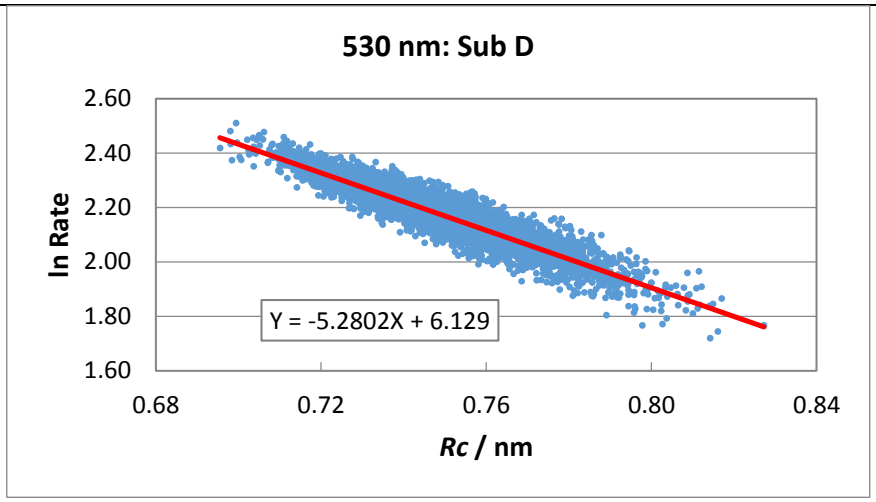

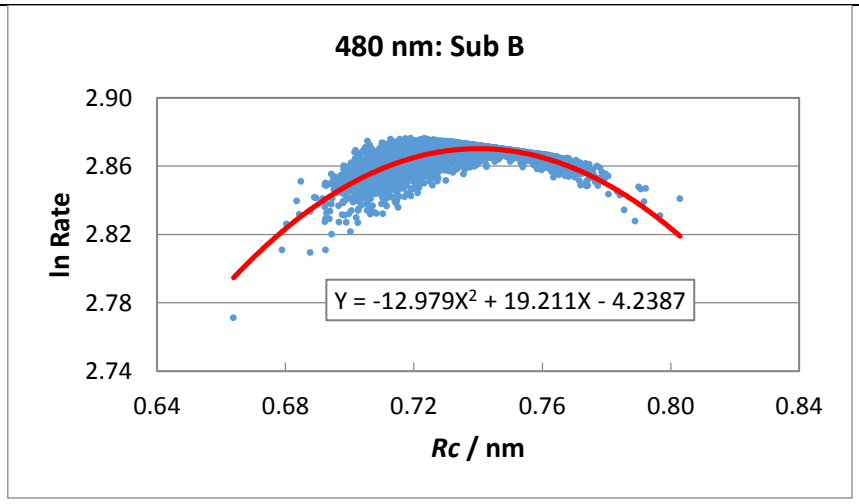

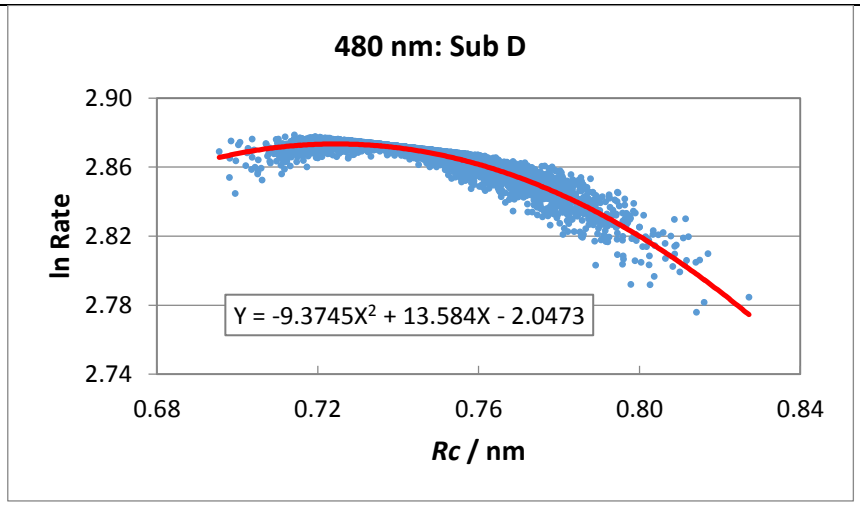

Figure 1 Relationship between ln Rate and *Rc* in Sub B and Sub D of P2O.

P2O consists of four subunits, Sub A, Sub B, Sub C and Sub D. Among these subunits, Sub B, Sub C and Sub D are the fast subunits with the fluorescence lifetimes of 0.11 ps at 530 nm and 0.057 ps at 480 nm, due to ET from Trp168 to Iso*.[62] ET rates are expressed in unit of ps^{-1}. Inserts indicate approximate functions of ln Rate (Y) and *Rc* (X). Physical quantities used were taken from Ref 38.

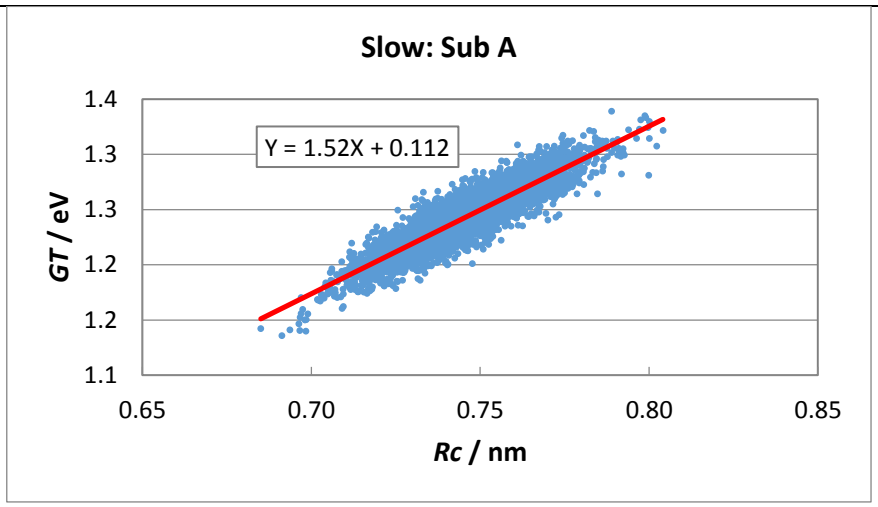

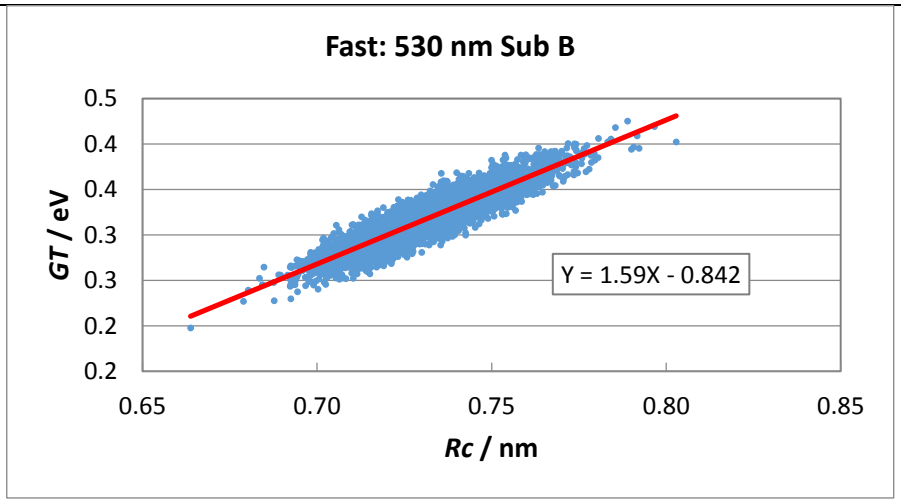

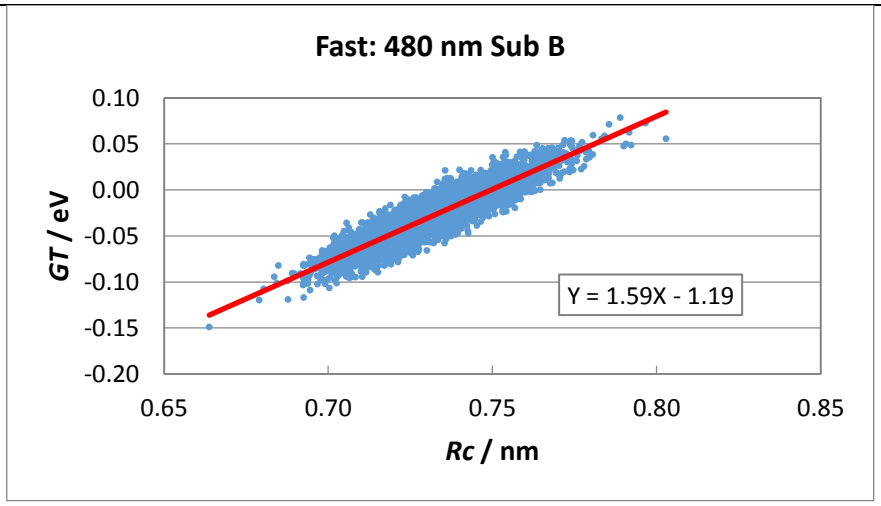

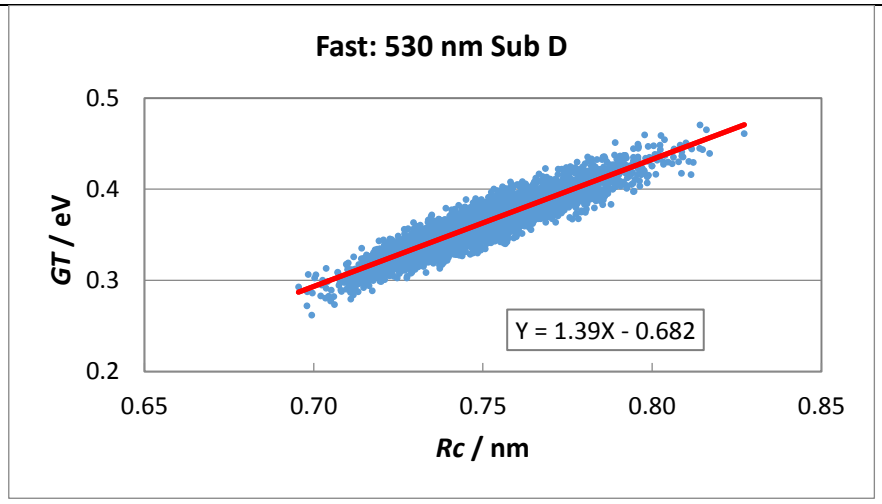

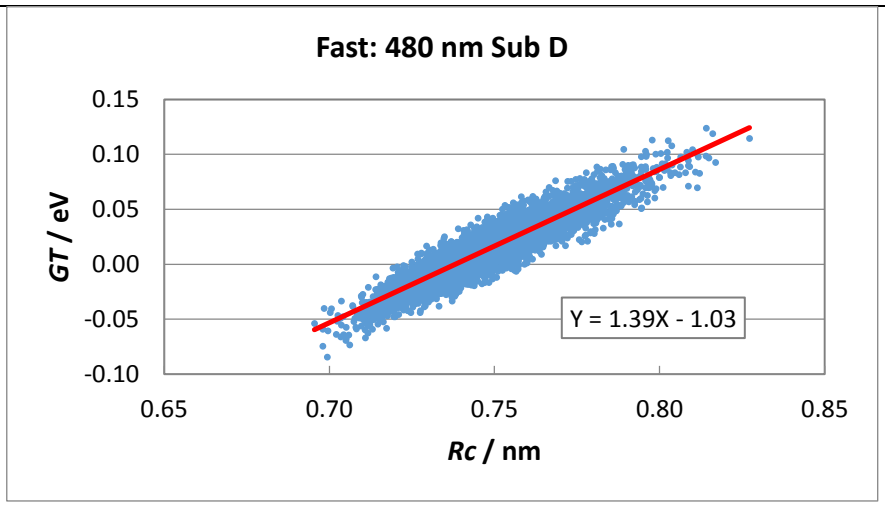

Figure 2 Dependence of *GT* on *Rc* in P2O.

The *GT* is defined by eq. 4 in text. Fluorescence lifetimes of Sub B are Sub D were 110 fs at 530 nm and 57 fs at 480 nm. Inserts indicate approximate functions of *GT* (Y) and *Rc* (X). Physical quantities used were taken from Ref 38.

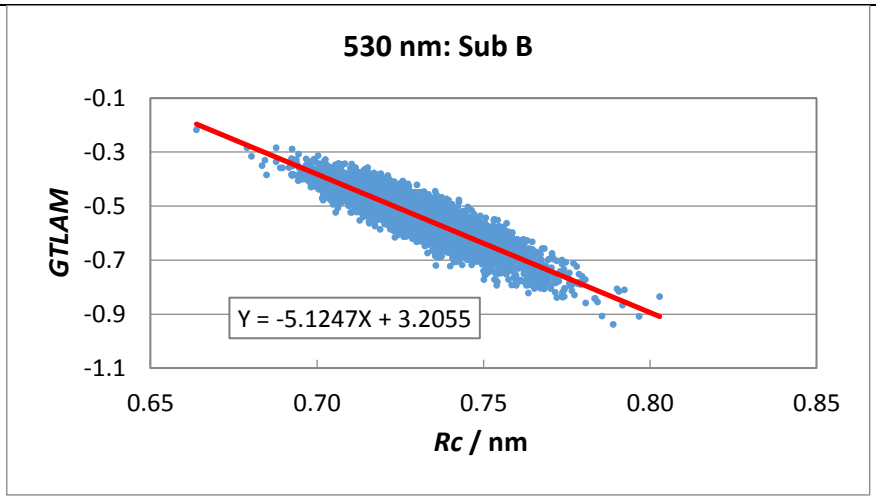

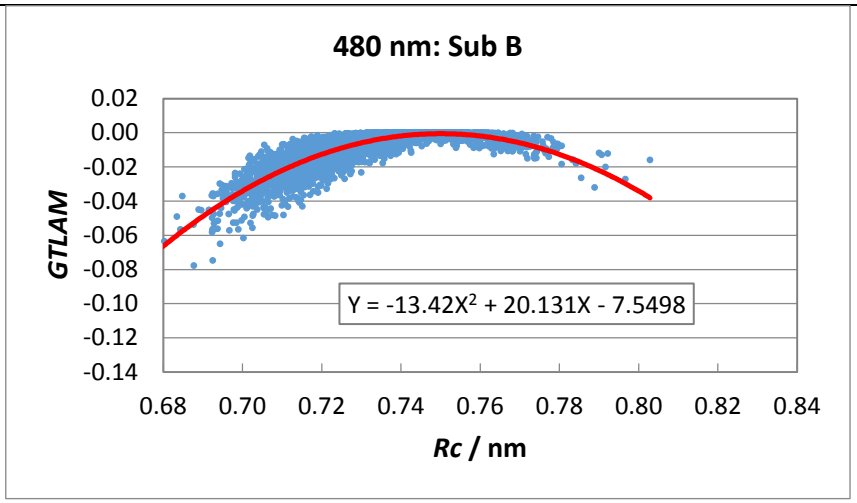

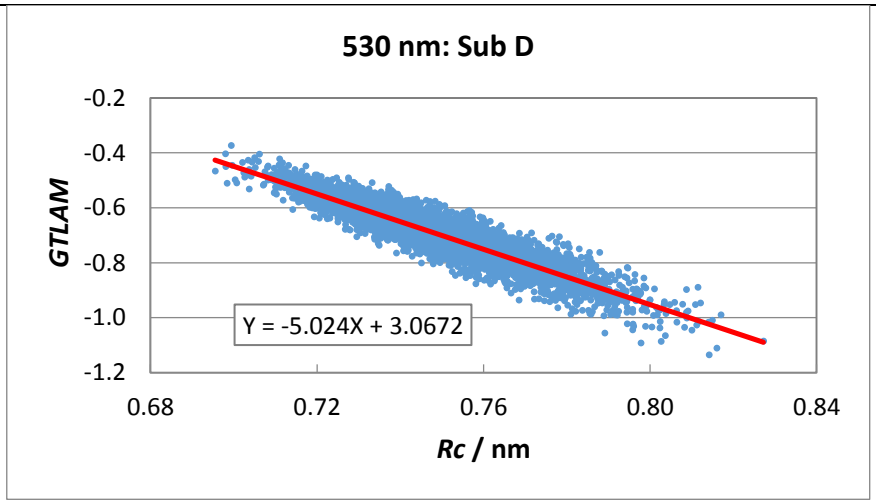

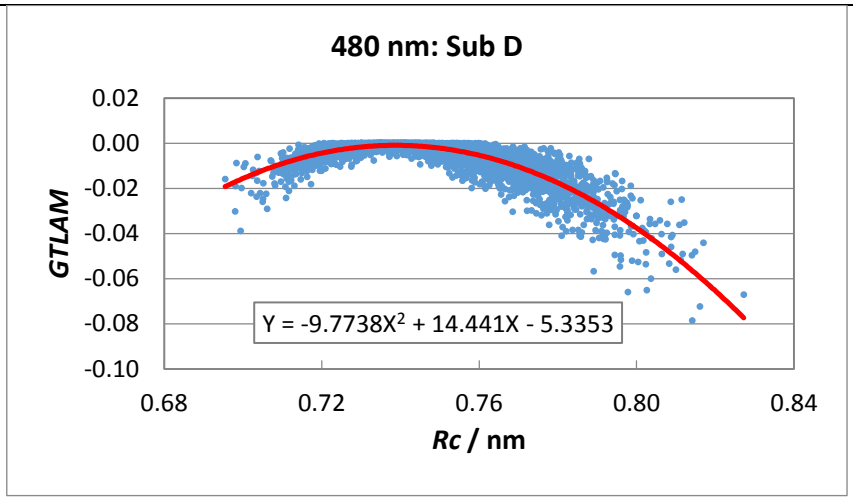

Figure 3 Relationship between *GTLAM* and *Rc* in P2O.

GTLAM is defined by eq. 5 in text. Inserts indicate approximate functions of *GTLAM* (Y) with *Rc* (X). Physical quantities used were taken from Ref 38.

A

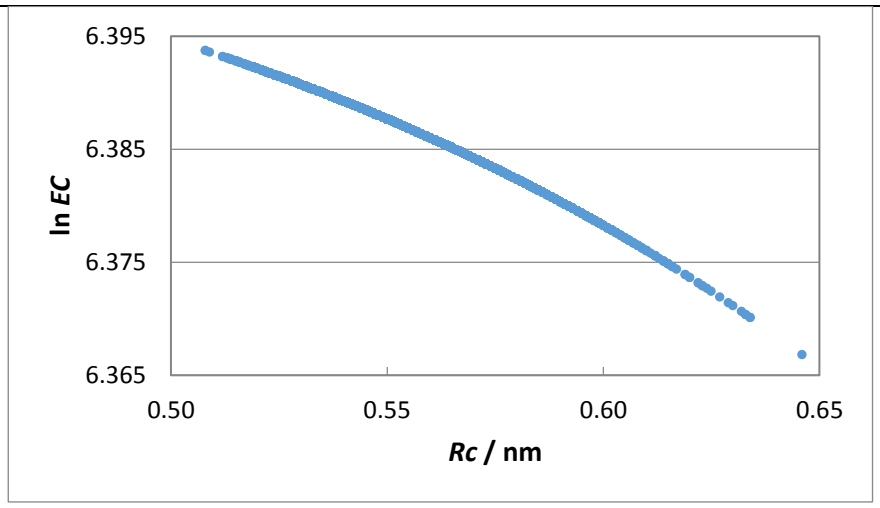

B

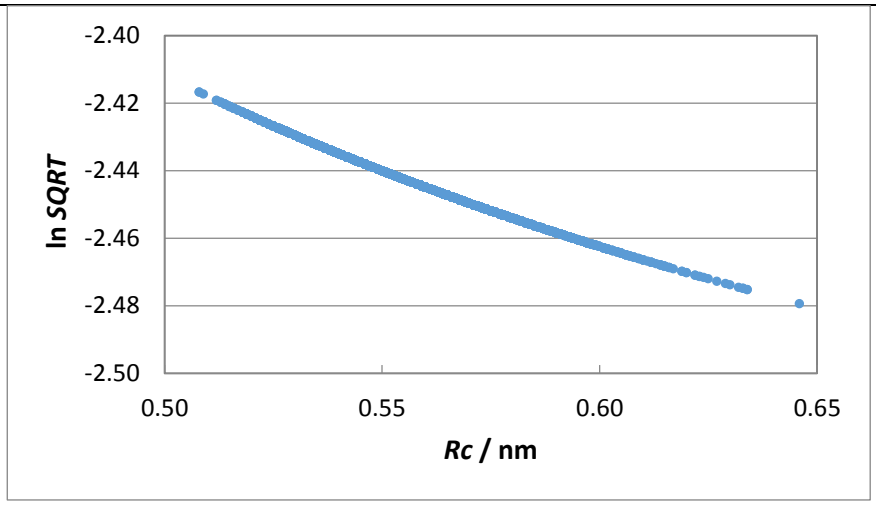

C

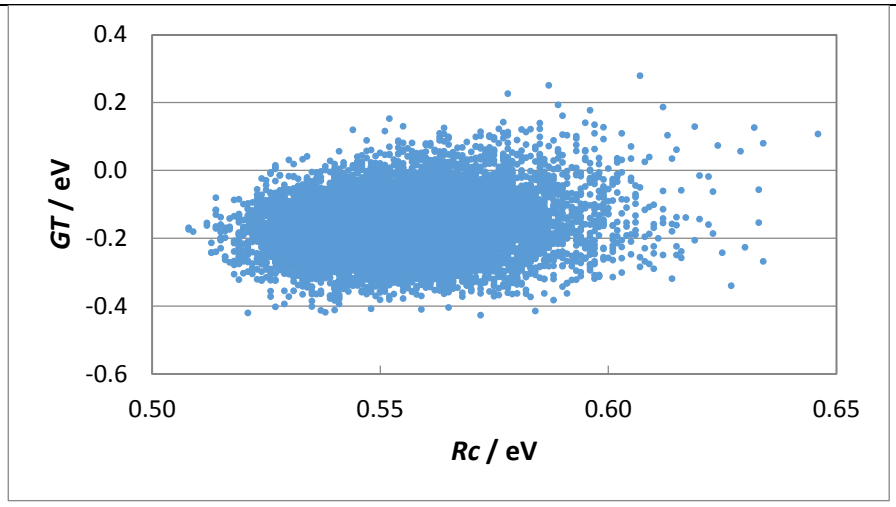

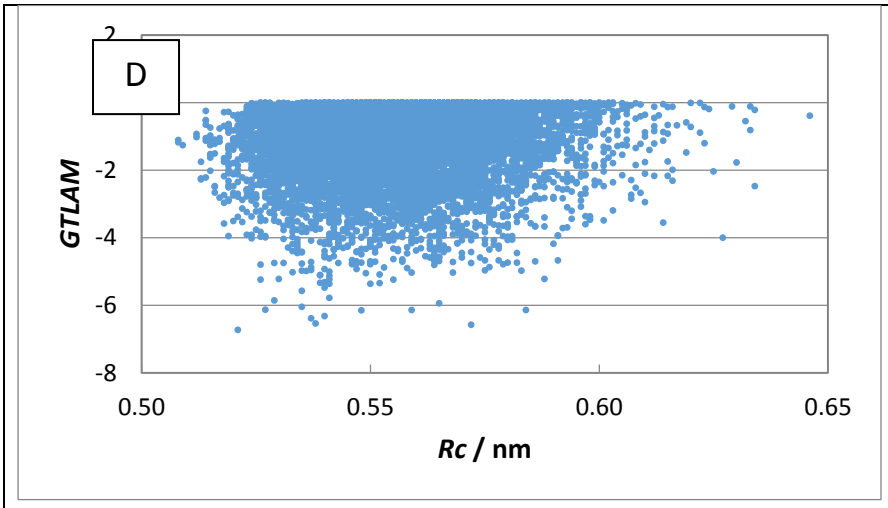

Figure 4 Dependence of the physical quantities related to ET rate of Tyr91 on *Rc* in HPFD.

Rc is distance between Tyr91 and Iso. Panel A shows ln *EC* vs *Rc* plot, panel B ln *SQRT* vs *Rc* plot, panel C *GT* vs *Rc* plot and panel D *GTLAM* vs *Rc* plot. Physical quantities used were taken from Ref 35.

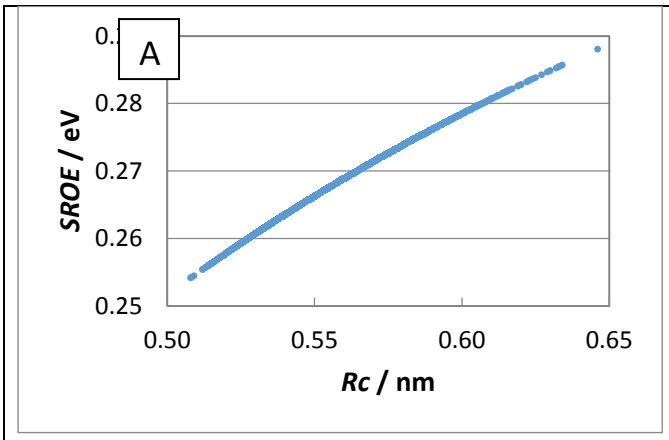

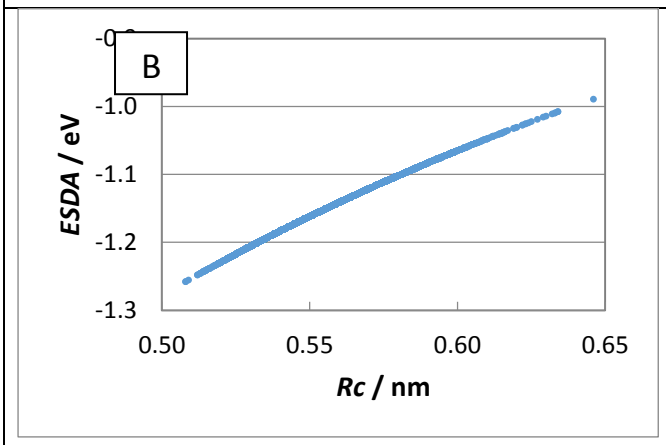

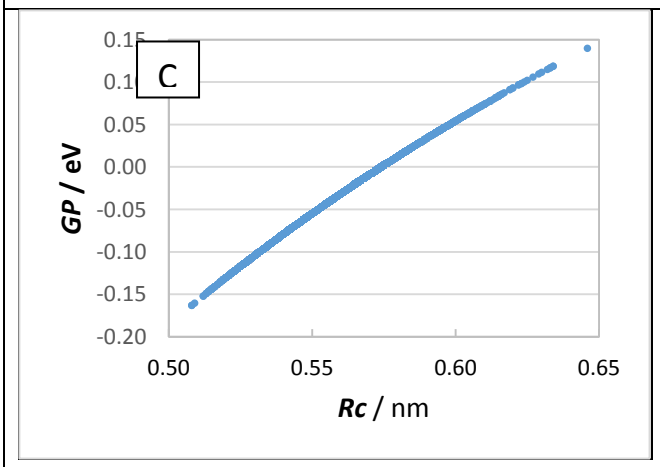

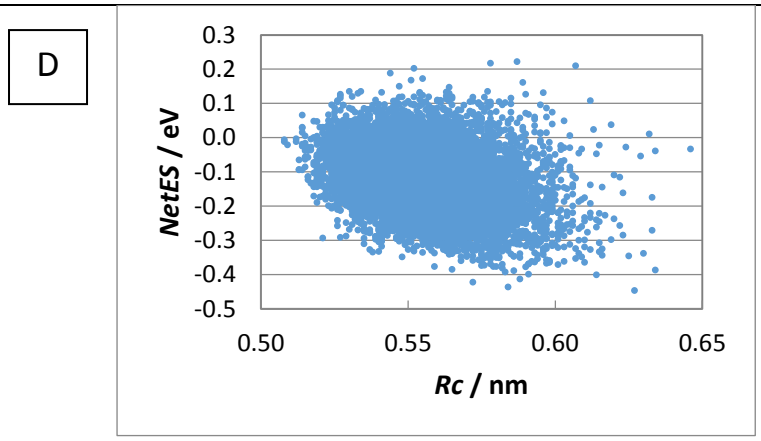

Figure 5 Dependence of individual component in *GT* term on *Rc* in HPFD.

Panel A indicates the relationship between *SROE* and *Rc*. Panel B between *ESDA* and *Rc*, Panel C between *GP* and *Rc*, and Panel D between *NetES* and *Rc*. *GP* is defined by eq. 6 in text. Physical quantities used were taken from Ref 35.

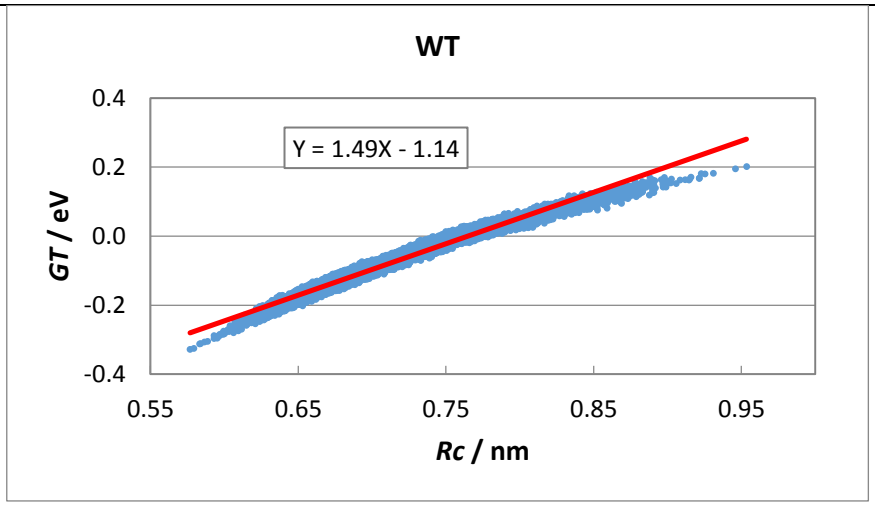

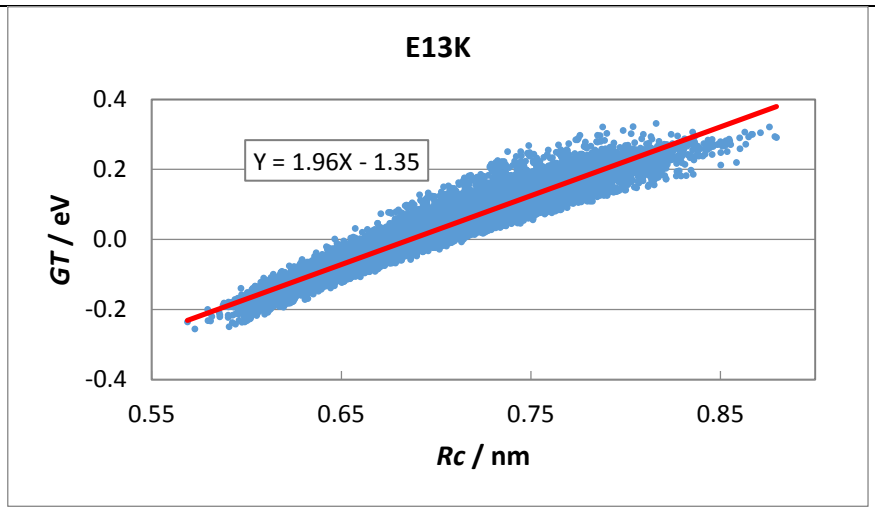

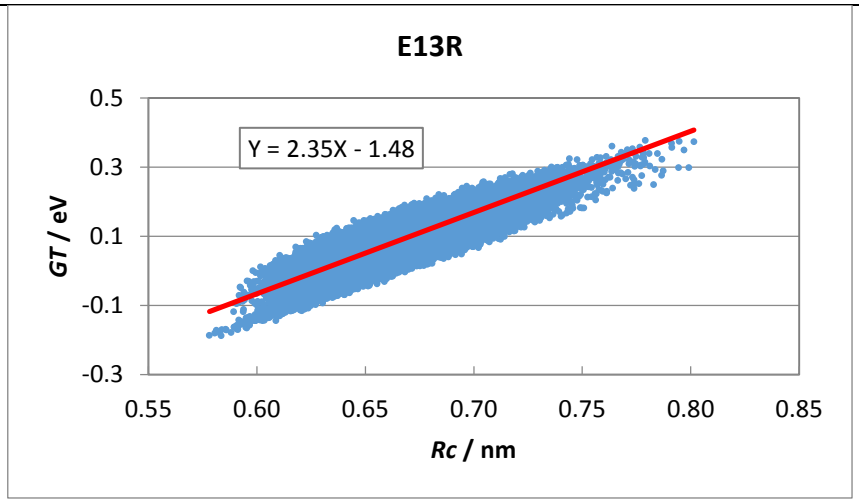

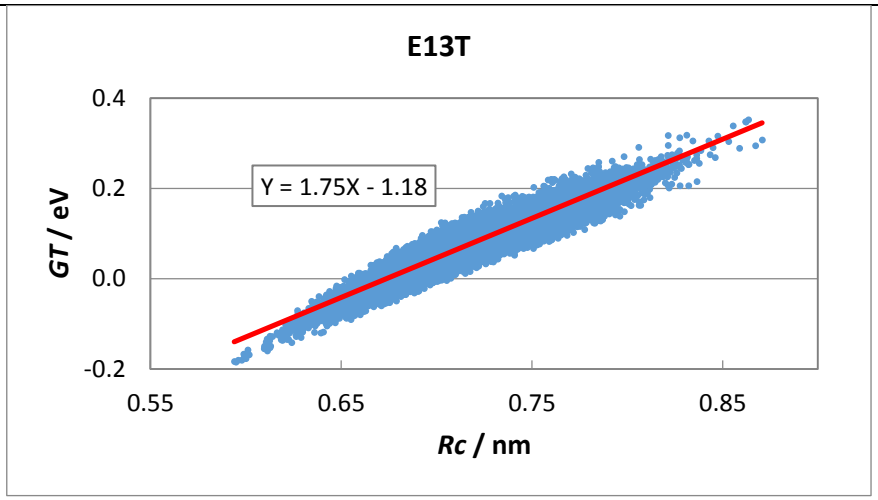

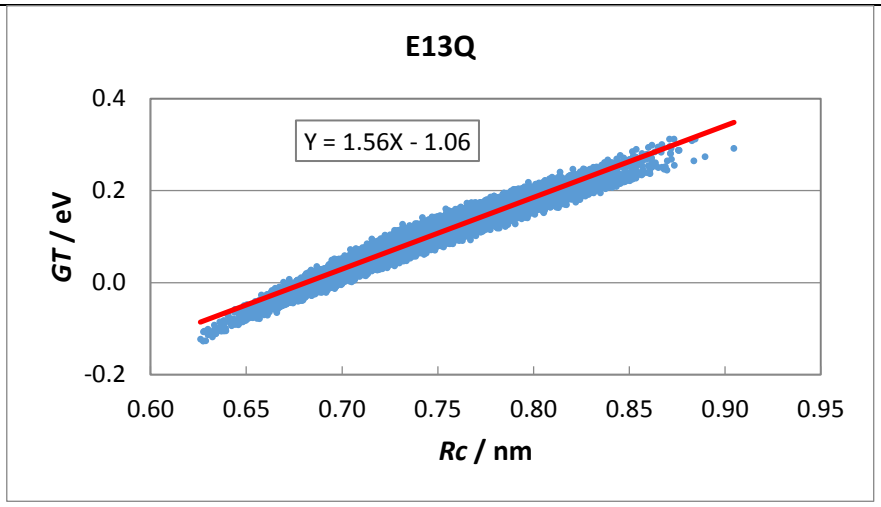

Figure 6 Relationship between *GT* and *Rc* of Trp32 in five FBP isoforms.

GT is defined by eq. 4 in text. Inserts indicate approximate function of *GT* (Y) with *Rc* (X).

Physical quantities used were taken from Refs 36 and 37.

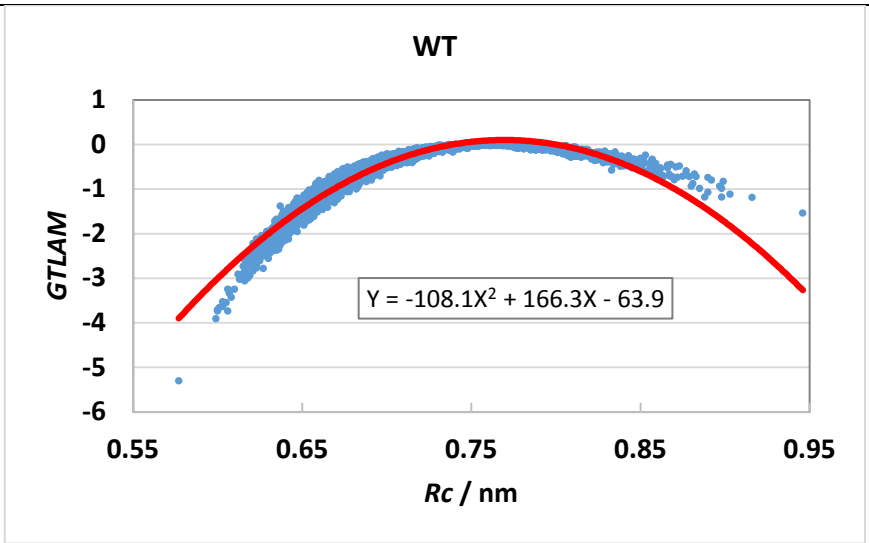

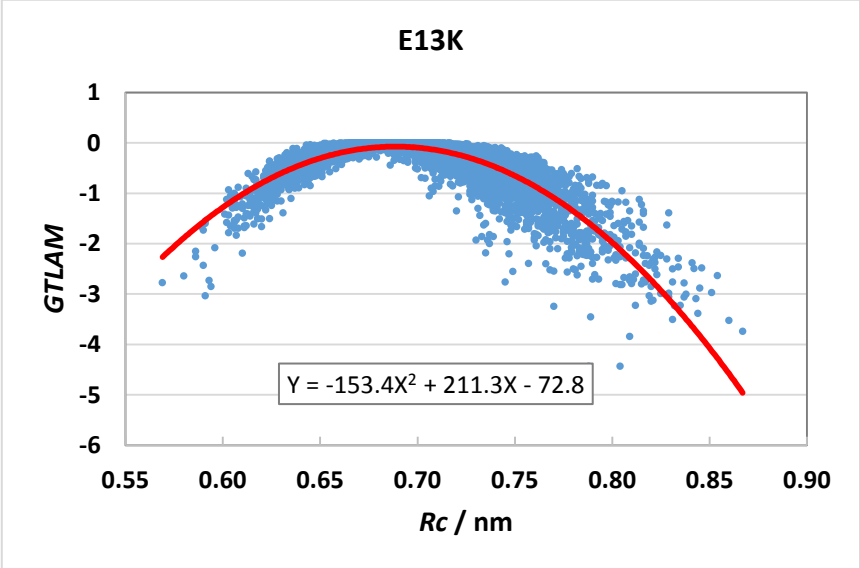

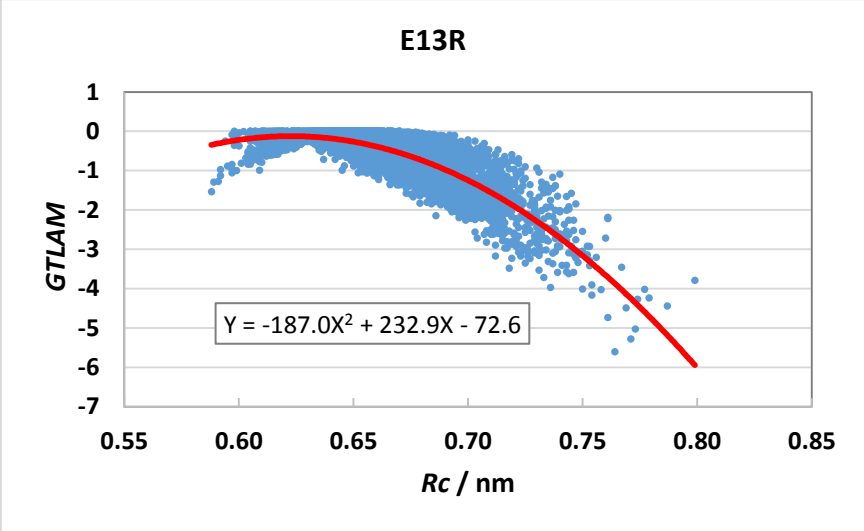

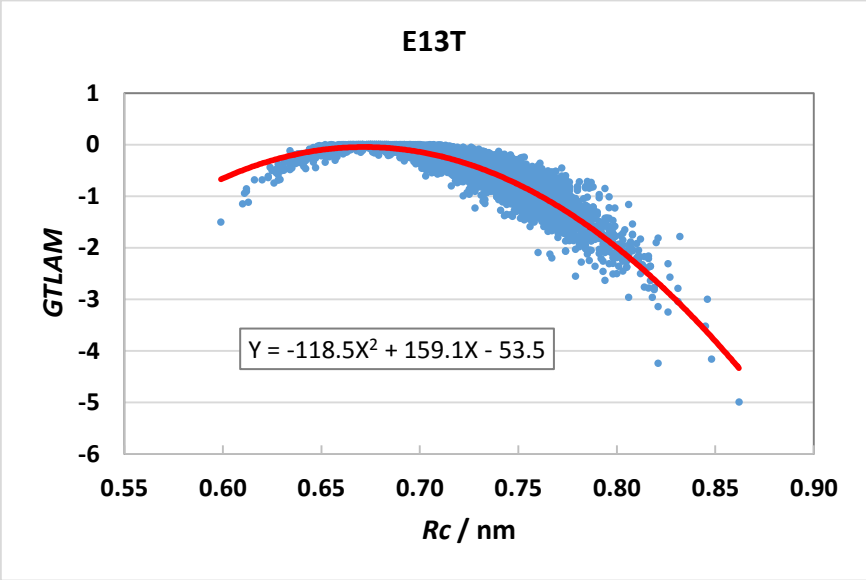

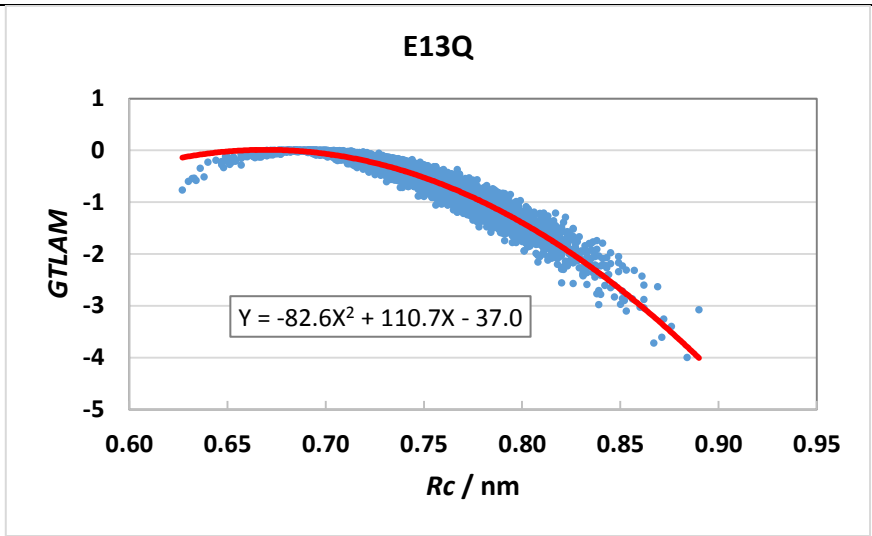

Figure 7 Relationship between *GTLAM* and *Rc* of Trp32 in five FBP isoforms. *GTLAM* is defined by eq. 5 in text. Inserts indicate approximate functions of *GTLAM* (Y) with *Rc* (X). Physical quantities used were taken from Refs 36 and 37.

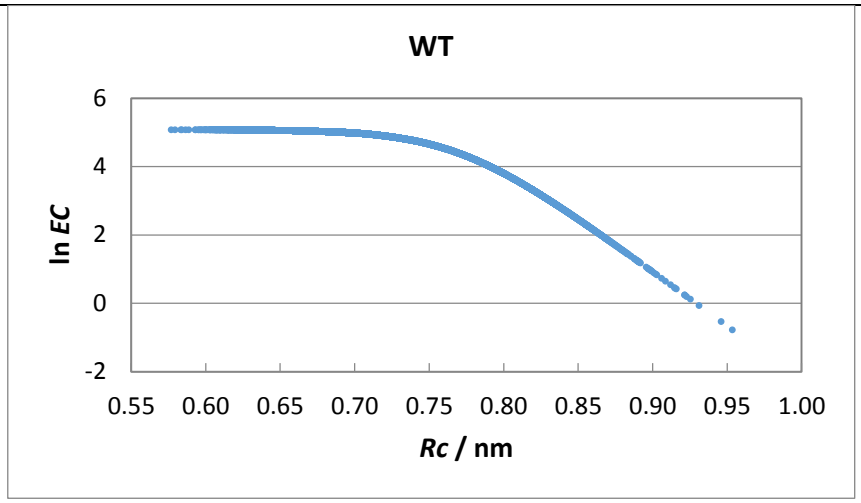

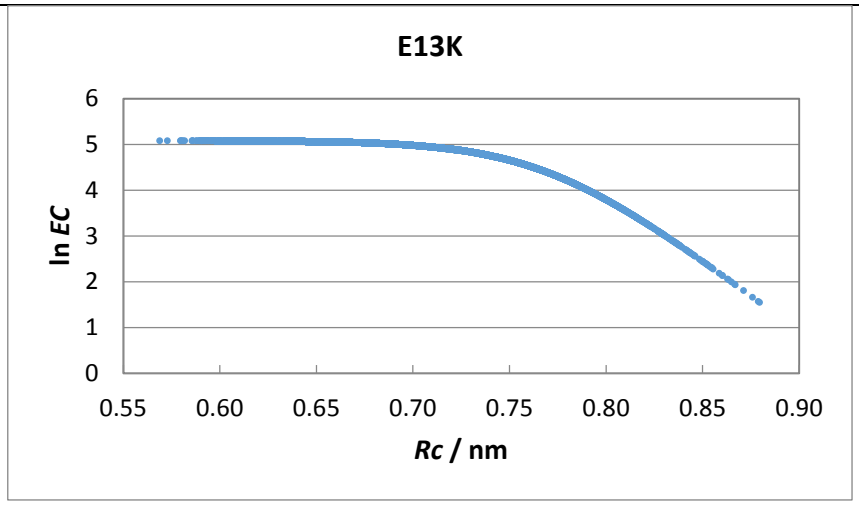

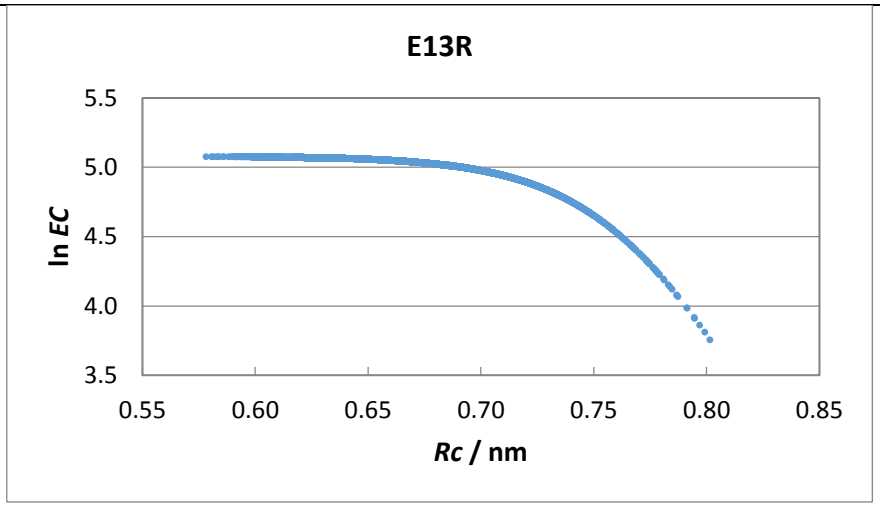

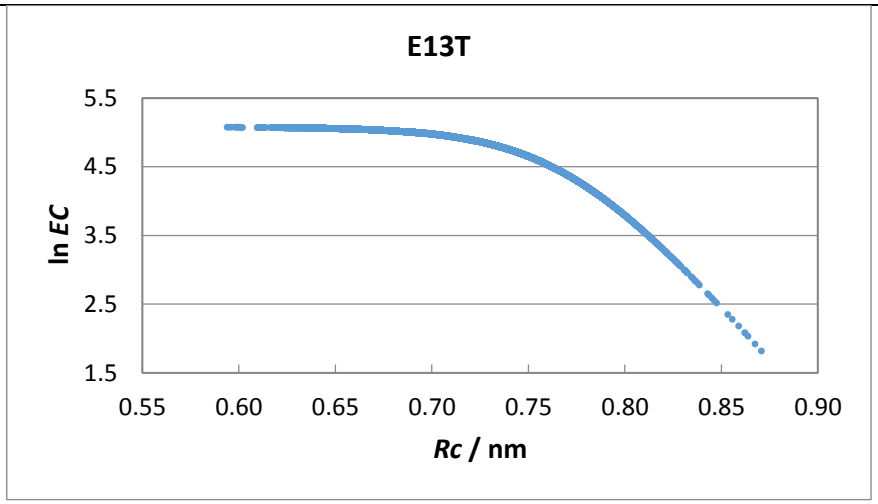

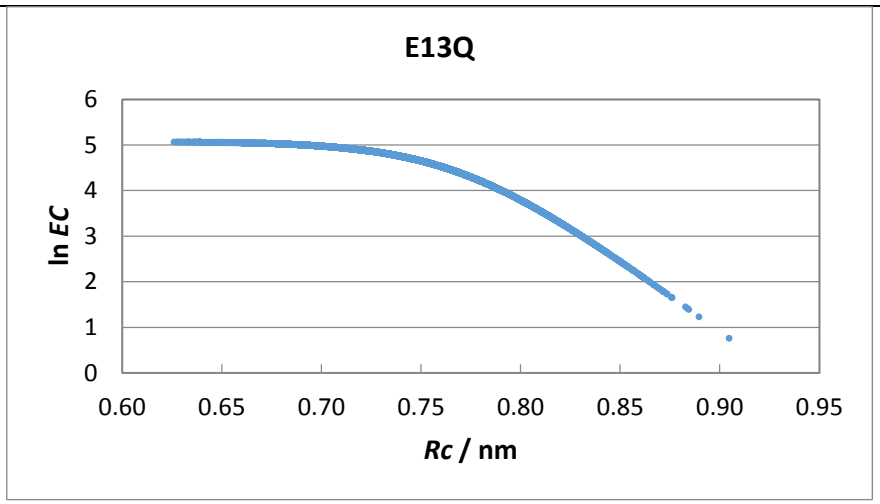

Figure 8 Relationship between logarithmic *EC* and *Rc* in five FBP isoforms.

The logarithmic *EC* is defined by eq. 2 in text. The ln *EC* linearly decreases with *Rc* longer than R_0 in all FBP isoforms, which shows ET process non-adiabatic in the region of *Rc*. Physical quantities used were taken from Refs 36 and 37.

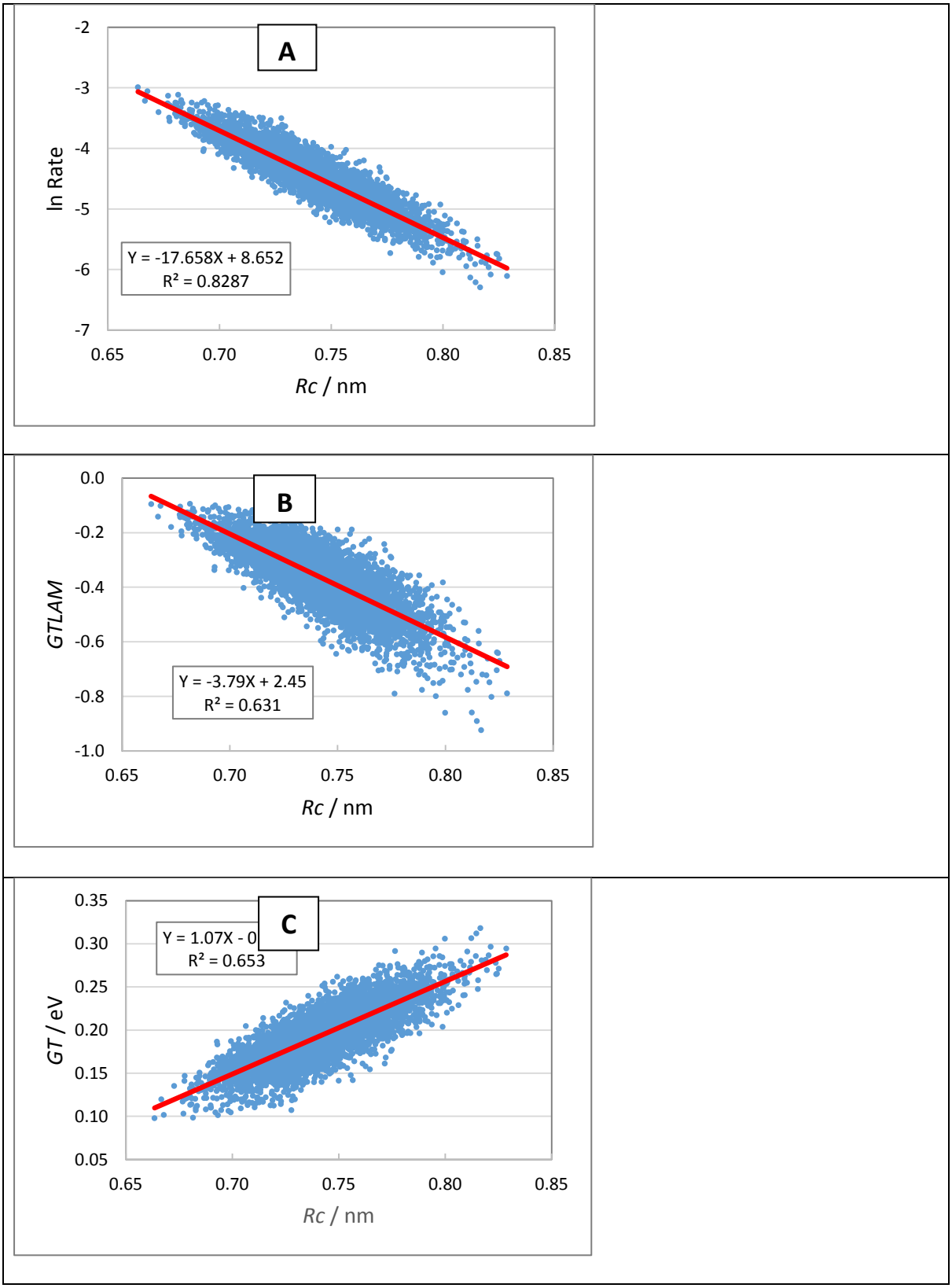

Figure 9 Dependencies of ln Rate, *GTLAM* and *GT* on *Rc* of Tyr224 at 10 °C in Sub A of DAAO dimer.

The ET rates are obtained with KM rate. *GTLAM* and *GT* are defined by eqs. 5 and 4 in text. Inserts indicate approximate linear functions and determination coefficients (R^2). Physical quantities used were taken from Ref. 60.

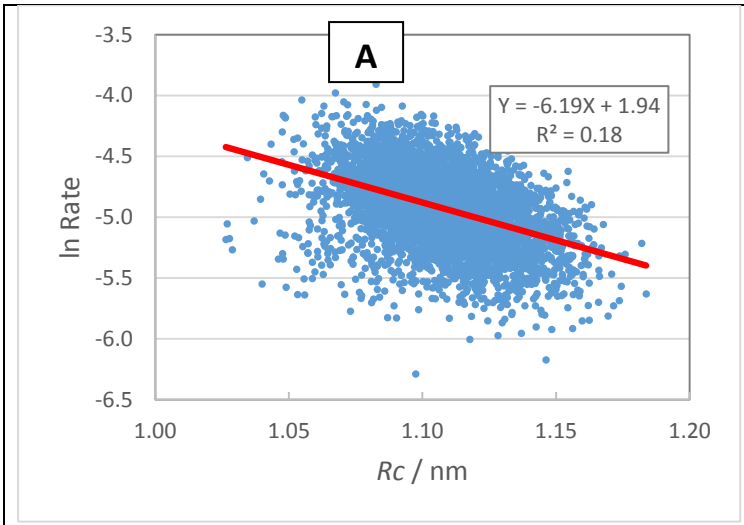

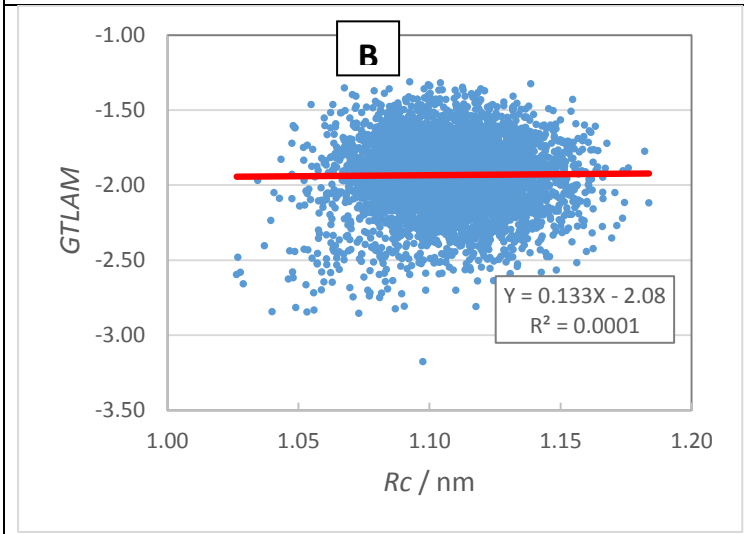

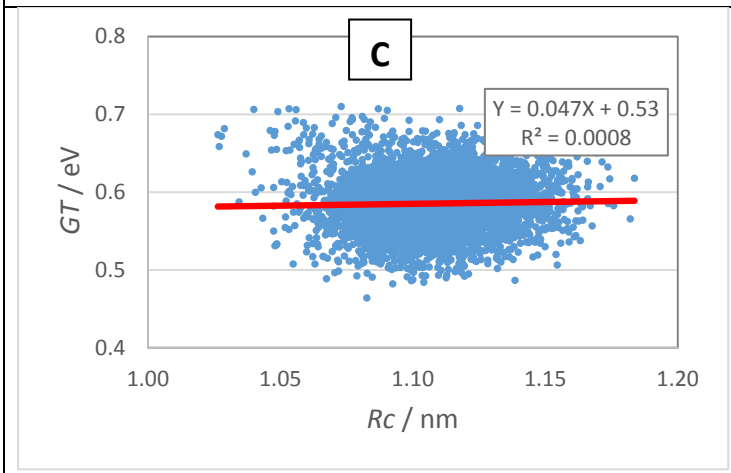

Figure 10 Dependencies of ln Rate, *GTLAM* and *GT* on *Rc* of Tyr314 at 10 °C in Sub A of DAAO dimer.

Inserts indicate approximate linear functions of Y (ln Rate in Panel A, *GTLAM* in Panel B, and *GT* in Panel C) with X (*Rc*). R^2 in the inserts represents determination coefficient. Physical quantities used are taken from Ref 60.

Table 1 Coefficients of approximate linear function of *GT* with *Rc* and range of *GT* in P2O

Wave-	Sub A		Sub B		Sub C		Sub D	
length (nm)	A (B)	Range	A (B)	Range	A (B)	Range	A (B)	Range
580	-	-	1.59	0.15 – 0.37	1.53	0.23 – 0.43	1.39	0.21 – 0.42
555	-	-	1.59	0.20 – 0.43	1.53	0.20 – 0.29	1.39	0.27 – 0.48
530	-	-	1.59	0.20 – 0.43	1.53	0.28 – 0.48	1.39	0.26 – 0.47
500	-	-	1.59	0.04 – 0.27	1.53	0.12 – 0.32	1.39	0.11 – 0.32
480	-	-	1.59	-0.15 – 0.08	1.53	-0.07 – 0.13	1.39	-0.08 – 0.12
-	1.52	1.14– 1.34	-	-	-	-	-	-

a The linear functions are expressed by Y = A X + B, where Y is *GT* and X is *Rc*.

Table 2 Coefficients of approximate functions of *GT* and *GTLAM* with *Rc* of Trp32 as ET donor in five FBP isoforms[a]

FBP	*GT*		*GTLAM*			ln Rate[b]		
	A	B	A	B	C	A	B	C
WT	1.49	-1.14	-108	167	-64.1	-185	270	-95.7
E13K	1.96	-1.35	-153	211	-72.8	-216	294	-97.2
E13R	2.35	-1.48	-187	233	-72.6	-213	269	-82.5
E13T	1.75	-1.18	-118	159	-53.5	-192	258	-84.1
E13Q	1.56	-1.06	-82.6	111	-37	-177	240	-79

a Approximate functions for *GT* was expressed by Y = AX + B, where Y is *GT* and X is *Rc*. Approximated functions for *GTLAM* and ln Rate are expressed by parabolic functions, $Y = AX^2 + B X + C$, where Y is *GTLAM* and X is *Rc*.

b Data were taken from Ref 36.

Table 3 The slope of linear function of physical quantities with *Rc* in Tyr224 and Tyr314 of DAAO dimer[a].

Subunit	Quantity	Tyr224		Tyr314	
(T / °C)		A[b]	R^{2c}	A[b]	R^{2c}
A (10)	ln Rate	-17.7	0.829	-6.19	0.174
	GTLAM	-3.79	0.631	0.133	0.0001
	GT	1.075	0.853	0.0465	0.0008
B (10)	ln Rate	-14.2	0.806	-7.61	0.478
	GTLAM	-2.94	0.5	-1.1	0.0265
	GT	0.704	0.541	0.234	0.0463
A (30)	ln Rate	-8.85	0.297	-6.38	0.278
	GTLAM	-0.747	0.0157	-0.07	0.00007
	GT	0.214	0.025	0.0686	0.0021
B (30)	ln Rate	-14.36	0.797	-8.64	0.496
	GTLAM	-2.88	0.495	-2.02	0.066
	GT	0.802	0.546	0.357	0.0998

a Data of ln Rate and *Rc* were taken from Ref 60.

b Slope in the linear functions of the quantities vs Rc.

c Determination coefficient (R^2) obtained as square of Pearson's correlation coefficient.

Table 4 Classification of the behavior on the relationship between logarithmic ET rate and *Rc*[a]

ln Rate (Lifetime)	Category[b]	*GP*[c]	*GT*[d] vs *Rc*	*GTLAM*[e] vs *Rc* (Slope)	ln Rate vs *Rc* Adiabatic (Slope)	Example	Non-adiabatic (Slope)	Example
Faster than 1 ps^{-1} (Shorter than 1 ps)	1)	» NetES	Linear around zero	parabolic	parabolic	Trp168 of fast subunits at 480 and 500 nm in P2O	Skewed parabolic	Trp32 in five FBP isoforms
	2)	« NetES	Scattered around zero	Scattered	No relation	Tyr91 in HPFD	Scattered linear (S_g)	-
Slower than 1 ps^{-1} (longer than 1 ps)	3)	» NetES	Linear with positive values	Linear ($-S_g$)	Linear ($-S_g$)	Trp168 in Sub A , and fast subunits at 530, 555, and 580 nm of P2O	Linear ($-S_g$-β)	Tyr35 in five FBP isoforms. Tyt224 and in DAAO dimer
	4)	« NetES	Scattered linear with positive values	Scattered linear ($-S_g$)	Scattered linear ($-S_g$)	-	Scattered linear ($-S_g$-β)	Tyr314 in DAAO dimer

a The behavior of ln Rate vs *Rc* relationship was observed with *Rc* fluctuations of MDS snapshots.

b see text.

c *GP* = *SROE* + *ESDA* + *SFEG* (eq. 6 in text) , where *SROE, ESDA,* and *SFEG* are solvent reorganization energy, electrostatic energy between Iso anion and a donor cation, and standard free energy gap.

d *GT* is given by eq. 4.

e *GTLAM* is given by eq. 5.